

# Distill and De-bias: Mitigating Bias in Face Recognition using Knowledge Distillation

Prithviraj Dhar<sup>1</sup>, Joshua Gleason<sup>2</sup>, Aniket Roy<sup>1</sup>, Carlos D. Castillo<sup>1</sup>, P. Jonathon Phillips<sup>3</sup>, Rama Chellappa<sup>1</sup>  
<sup>1</sup>Johns Hopkins University, <sup>2</sup>University of Maryland, College Park, <sup>3</sup>NIST

{pdhar1, aroy28, carlosdc, rchella4}@jhu.edu, gleason@umd.edu, jonathon.phillips@nist.gov

## Abstract

Face recognition networks generally demonstrate bias with respect to sensitive attributes like gender, skintone etc. For gender and skintone, we observe that the regions of the face that a network attends to vary by the category of an attribute. This might contribute to bias. Building on this intuition, we propose a novel distillation-based approach called *Distill and De-bias (D&D)* to enforce a network to attend to similar face regions, irrespective of the attribute category. In *D&D*, we train a teacher network on images from one category of an attribute; e.g. light skintone. Then distilling information from the teacher, we train a student network on images of the remaining category; e.g., dark skintone. A feature-level distillation loss constrains the student network to generate teacher-like representations. This allows the student network to attend to similar face regions for all attribute categories and enables it to reduce bias. We also propose a second distillation step on top of *D&D*, called *D&D++*. For the *D&D++* network, we distill the ‘un-biasedness’ of the *D&D* network into a new student network, the *D&D++* network. We train the new network on all attribute categories; e.g., both light and dark skintones. This helps us train a network that is less biased for an attribute, while obtaining higher face verification performance than *D&D*. We show that *D&D++* outperforms existing baselines in reducing gender and skintone bias on the IJB-C dataset, while obtaining higher face verification performance than existing adversarial de-biasing methods. We evaluate the effectiveness of our proposed methods on two state-of-the-art face recognition networks: *Crystalface* and *ArcFace*.

## 1. Introduction

The accuracy of face recognition networks [11, 13, 38, 45, 53] has significantly improved in the last few years. Because of this, such face recognition systems are being used in a large number of applications. This has raised concerns

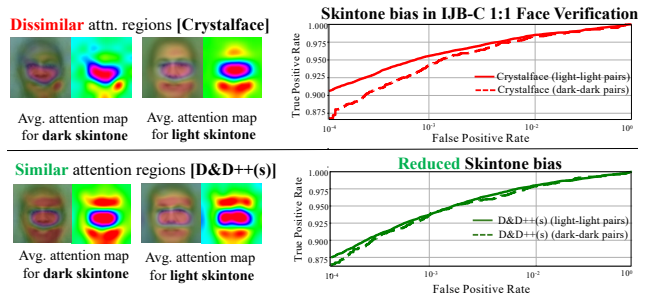


Figure 1. (**Top row**) Face recognition networks attend to different spatial regions in faces, depending on protected attributes (here, shown for skintone attribute). Here, we show the average attention maps generated using the pre-trained *Crystalface* network for frontal faces with light and dark skintone. This difference in processing faces with light and dark skintone might contribute to skintone bias. (**Bottom row**) Our proposed method *D&D++* enforces a network to attend to similar spatial regions for both light and dark skintones, and consequently reduces skintone bias. We report similar findings with respect to the gender attribute.

about bias against sensitive attributes such as age, gender or race. A recent study from NIST [23] has shown that characteristics such as gender and ethnicity impact the verification and matching performance of existing algorithms. Several works [5, 9, 32, 33, 40, 43, 57] have explored the issue of bias against gender, race and skintone in face recognition.

A possible approach to mitigate gender or skintone bias would be to re-train a large scale face recognition network on a dataset which is balanced in terms of these attributes. However, as shown in [3, 16, 58], training a network on a balanced dataset does not always lead to unbiased systems. [16] points out that while we can balance the dataset in terms of gender or skintone, there exists appearance variation between demographic subgroups with respect to multiple factors such as pose, illumination etc., which may lead to a biased system. Some works [15, 21] have proposed adversarial strategies to prevent face recognition networks from encoding sensitive attributes like gender and race. However, since gender and race are integral to the face identity, removing such attributes from face recognition features generally reduces their face verification accu-

racy. Among non-adversarial methods, GAC [22] proposes an adaptive filtering technique to mitigate racial bias. However, the effectiveness of GAC applied to other attributes (such as gender) is currently unclear. Similar to GAC, we propose non-adversarial techniques to mitigate bias in face recognition. More specifically, we present two novel knowledge distillation-based techniques called D&D and D&D++ to incrementally learn different categories of a given sensitive attribute while significantly reducing bias with respect to that attribute. We show that our proposed methods can be used to reduce bias with respect to either gender or skintone, and are therefore likely to generalize for other attributes. Our methods also generalize to different face recognition models.

Buolamwini *et al.* [8] introduced skintone as an alternative to race. It can be difficult to quantify the race category of multi-racial faces. Skintone, on the other hand, is more scientifically defined by the Fitzpatrick scale [20]. Therefore, following previous works [15, 36], we have opted to mitigate skintone bias, as opposed to racial bias. In summary, we make the following contributions in our work:

1. We observe that face recognition networks attend to different regions of the face, depending on the gender or skintone category. We illustrate this observation with GradCAM [52] generated attention maps (Figs. 1,3,6, Section 5.4.1). These differences in how algorithms process faces from different demographic categories may lead to bias in face recognition.
2. Building on this observation, we propose a method, called **Distill and De-bias (D&D)**, that enforces a network to attend to similar spatial regions in both male and female faces (and in both faces with light and dark skintones). We show the ability of D&D to reduce gender and skintone bias in two state-of-the-art face recognition networks: Crystalface [45] and ArcFace [11]. To the best of our knowledge, *we are the first to use knowledge distillation for designing bias mitigation strategies in face recognition.*
3. We propose D&D++ to further improve the face verification performance, while inheriting the ‘unbiasedness’ of D&D. D&D++, while being de-biased, achieves higher face verification performance than state-of-the-art adversarial de-biasing methods on the IJB-C [37] dataset.

## 2. Related Work

**Bias in face recognition:** Empirical studies [8, 19, 23, 39, 44] have shown that many publicly available systems performing face recognition or face analysis demonstrate bias towards sensitive attributes such as race and gender. With respect to gender bias, [3, 36] show that the performance of face recognition on females is lower than that of

Method	Target task	Sensitive attribute
[4]	Gender/Age pred.	Age/Gender
[34]	Smile, high-cheeks	Gender, make-up
[5]	Face detection	Skintone
[57]	Face recognition	Race
[59]	Expression pred.	Age, gender, race
[21]	Face recognition	Age, gender, race
[41]	Attractiveness pred.	Gender, age
[50]	Face recognition	Gender, race
[15]	Face recognition	Gender, skintone

Table 1. Methods that adversarially remove sensitive attributes to reduce bias with respect to these attributes in the target task.

males. Use of cosmetics by females [10, 31] and gendered hairstyles [1] has been assumed to play a major role in the resulting gender bias. However, [2] shows that cosmetics only play a minor role in the gender gap. [22, 56, 57, 61] explore the issue of racial bias in face recognition, and propose strategies to mitigate the same. [36] shows that face verification systems perform better on lighter skintones than darker skintones. [12, 29] show that face recognition networks implicitly encode information about sensitive attributes during training, which might lead to bias w.r.t these attributes.

**Building fairer datasets:** It has been speculated that the imbalanced training datasets might lead to bias in face recognition. However, [3] shows that the gender bias is not mitigated when equal number of male and female identities are used for training. [26] introduces a dataset to measure the robustness of AI models to a diverse set of genders and skintones. Similarly, [49] presents an evaluation dataset that is balanced in terms of race and gender and provides the verification protocol for the same.

**Adversarial de-biasing:** Several researchers have proposed adversarial strategies to reduce the encoding of sensitive attributes (to reduce the bias with respect to these attributes), while performing a face-based target task. We provide a brief summary of these works in Table 1. [15, 21, 41] have reported that the face verification performance of the adversarially-debiased systems in the target task decreases due to the removal of sensitive attributes such as gender.

**Knowledge distillation (KD):** KD [30] has been primarily applied to continual learning tasks [35, 47]. In a KD framework, a student network (initialized using a pre-trained teacher network) is trained to learn new classes or tasks that are not recognizable by the teacher network, and mimic the output score distribution of the teacher model for preventing forgetting of the classes/tasks that the teacher network was trained on. Several works [18, 51, 63] have shown that directly matching feature activations of teacher and student networks from their intermediate layers is also an effective way to distill the teacher’s knowledge into the student. Inspired by this, we employ feature-level KD in our work to enforce a student trained on a specific attribute category (e.g. males) to mimic a teacher that is trained on a different attribute category (e.g. females).

### 3. Problem Statement

Given a binary face attribute  $A$  with categories  $a_1$  and  $a_2$ , our goal is to enforce a network to process faces with  $A = a_1$  and  $A = a_2$  in a similar way. We hypothesize that a network that processes faces with attribute  $A = a_1$  and faces with attribute  $A = a_2$  in a similar way will demonstrate lower bias with respect to attribute  $A$ . For attribute  $A = \text{skintone}$ ,  $(a_1, a_2) = (\text{Light}, \text{Dark})$ . For attribute  $A = \text{gender}$ ,  $(a_1, a_2) = (\text{Female}, \text{Male})$ .

**Bias measure:** Following [15], we define gender and skintone bias, at a given false positive rate (FPR) as follows:

$$\text{Gender Bias}^{(F)} = |\text{TPR}_m^{(F)} - \text{TPR}_f^{(F)}| \quad (1)$$

$$\text{Skintone Bias}^{(F)} = |\text{TPR}_l^{(F)} - \text{TPR}_d^{(F)}| \quad (2)$$

where  $(\text{TPR}_m^{(F)}, \text{TPR}_f^{(F)}, \text{TPR}_l^{(F)}, \text{TPR}_d^{(F)})$  denote the true positive rates for the verification of male-male, female-female, light-light and dark-dark pairs respectively at FPR  $F$ . Our goal is to train face recognition networks that reduce the bias (Eq. 1 or 2), while maintaining reasonable face verification performance in face verification. The reasoning for using this measure instead of difference between AUC or EER is provided in [15].

**Measuring bias/performance trade-off:** We also adopt the tradeoff measure called *bias performance coefficient* (BPC) from [15]. This is a measure of the trade-off between bias reduction and drop in face verification performance and is defined as

$$\text{BPC}^{(F)} = \frac{\text{Bias}^{(F)} - \text{Bias}_{deb}^{(F)}}{\text{Bias}^{(F)}} - \frac{\text{TPR}^{(F)} - \text{TPR}_{deb}^{(F)}}{\text{TPR}^{(F)}}. \quad (3)$$

Here,  $(\text{TPR}^{(F)}, \text{Bias}^{(F)})$  refer to the *overall* TPR obtained by original features and the corresponding bias (Gender/Skintone bias) at FPR of  $F$ .  $(\text{TPR}_{deb}^{(F)}, \text{Bias}_{deb}^{(F)})$  denote their de-biased counterparts. We aim to build systems that achieve high BPC values, since a higher BPC denotes high bias reduction and low drop in face verification performance. The original network (without any de-biasing) would have a zero BPC (since  $\text{Bias}^{(F)} = \text{Bias}_{deb}^{(F)}$  and  $\text{TPR}^{(F)} = \text{TPR}_{deb}^{(F)}$ ). We note that a system with  $\text{TPR}_{deb}^{(F)} \gg \text{TPR}^{(F)}$  and  $\text{Bias}_{deb}^{(F)} > \text{Bias}^{(F)}$  can have a high BPC value, which is not desirable. But, as pointed out in [15], most de-biasing systems have  $\text{TPR}_{deb}^{(F)} < \text{TPR}^{(F)}$  and  $\text{Bias}_{deb}^{(F)} < \text{Bias}^{(F)}$ . An ideal system that reduces the bias to 0 and does not reduce the TPR will have  $\text{BPC} = 1$ . A negative BPC denotes that the percentage drop in TPR is higher than the percentage reduction in bias. We denote the BPC for skintone as ‘BPC<sub>st</sub>’ and that for gender as ‘BPC<sub>g</sub>’.

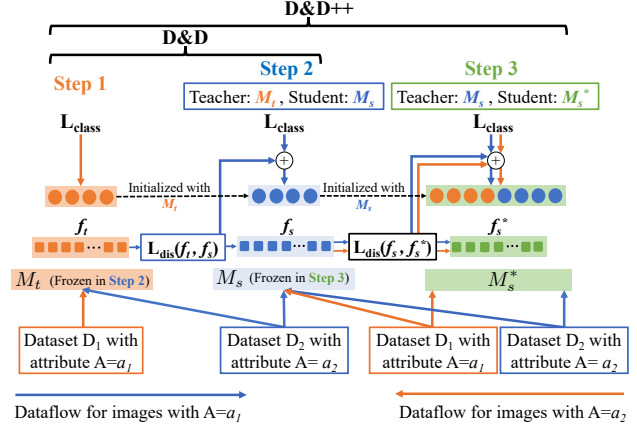


Figure 2. Proposed approach. **Step 1:** We train  $M_t$  on faces with  $A = a_1$ . **Step 2 (D&D):** We initialize  $M_s$  using  $M_t$  and train it using faces with  $A = a_2$ . Here,  $M_s$  is enforced to generate teacher-like features using  $L_{dis}$ , and thus process faces belonging any attribute category ( $a_1$  or  $a_2$ ) in a similar way. **Step 3 (D&D++):** We initialize a new student network  $M_s^*$  using  $M_s$ .  $M_s^*$  is trained on the entire dataset to improve its recognition performance, while it inherits the ‘unbiasedness’ of  $M_s$  using  $L_{dis}$ .

## 4. Proposed approach

### 4.1. Motivation

Let us consider a binary face attribute  $A$  with two categories:  $a_1$  and  $a_2$ . Suppose that we have a face image  $I_1$ , with attribute  $A = a_1$  and image  $I_2$  with attribute  $A = a_2$ . We hypothesize that a relatively unbiased face recognition network must attend to similar facial regions for both  $I_1$  and  $I_2$ , irrespective of their attribute  $A$  categories. However, our initial experiments show that the spatial regions that a network attends to vary for different genders (Figs. 3a, 6a-first row), and for different skintones (Figs. 3b, 6b-first row). A network that does not attend to similar face regions for males and females (or faces with light and dark skintones) in a similar way might exhibit bias, as shown in Fig. 1 (top row). More details regarding these results are presented in Section 5.4.1. From these results, it appears that male and female images are processed differently by a face recognition network. Similarly, images with light and dark skintones are also processed differently. Therefore, we propose KD-based methods that enforce a network to process faces from all attribute categories in a similar way, so that the network attends to similar regions of the face, irrespective of the attribute category.

### 4.2. Distill and De-bias (D&D) and D&D++

Here, we explain the steps in D&D and D&D++ (Fig. 2): **Step 1:** We train the teacher network  $M_t$  using faces with attribute  $A = a_1$ .

**Step 2 (Feature-level knowledge distillation - D&D):** We initialize a student network  $M_s$  using  $M_t$ , and train it using images with  $A = a_2$ . Let  $I$  be such an image with  $A = a_2$ .

$I$  is fed to both  $M_t$  and  $M_s$ , to obtain features  $f_t$  and  $f_s$ , extracted from the penultimate layer of the corresponding networks. To enforce the student  $M_s$  to mimic  $M_t$ 's way of processing faces, we employ feature-level knowledge distillation to distill  $M_t$ 's knowledge of processing faces into  $M_s$ . We define the distillation loss  $L_{dis}$  as

$$L_{dis}(f_s, f_t) = 1 - \frac{f_s \cdot f_t}{\|f_s\| \|f_t\|}. \quad (4)$$

To constrain  $M_s$  to process a face like  $M_t$  would, we minimize the cosine distance between  $f_t$  and  $f_s$  using  $L_{dis}$ . Our application of feature-level KD is inspired by [51]. Note that we do not apply KD on the output scores as done in [35], since face verification protocols like [37] use the face recognition features from the penultimate layer (and not the output score vector). Additionally, we would like  $M_s$  to classify identities using  $L_{class}$ . This is the standard cross-entropy loss. Combining these constraints, we train  $M_s$  using the bias reducing classification loss  $L_{br}$  as

$$L_{br} = L_{class} + \lambda_1 L_{dis}, \quad (5)$$

where  $\lambda_1$  is used to weight  $L_{dis}$ . In this step, the teacher  $M_t$  remains frozen. The distillation step helps in two ways:

1.  $M_s$  is initialized with  $M_t$  (which was trained on faces with  $A = a_1$ ) and  $L_{dis}$  prevents  $M_s$  from diverging too much from  $M_t$ . Therefore, *the distillation step allows  $M_s$  to process faces with  $A = a_1$  in the same way  $M_t$  would process them, even though  $M_s$  is never trained on images from  $a_1$  category.*
2.  $M_t$  is never trained on faces with  $A = a_2$ . So,  $L_{class}$  allows  $M_s$  to classify faces from  $a_2$  category. But,  $L_{dis}$  enforces  $M_s$  to process faces from  $a_2$  category in the same way  $M_t$  and  $M_s$  would process faces from  $a_1$  category.

In this way,  $M_s$  can process faces from both  $a_1$  and  $a_2$  categories as  $M_t$  would process faces from  $a_1$  category. As a result,  $M_s$  learns to attend to similar face regions for faces belonging to any category of attribute  $A$ , as shown in Figs. 3, 6. Consequently, we find that  $M_s$  is able to significantly reduce bias with respect to attribute  $A$  (Sec. 5.4.2). For inference, we extract features from the penultimate layer of the trained  $M_s$  network for the evaluation dataset, and perform 1:1 face verification. We note that, while  $M_s$  considerably reduces bias in face verification, it obtains lower overall face verification performance (Sec. 5.4.2). We believe this is because neither  $M_s$  nor its teacher  $M_t$  is ever trained on the entire dataset. Hence, *we train a new student  $M_s^*$  (initialized with  $M_s$ ) on the entire dataset to improve the identity classifying ability of  $M_s$ , while distilling the ‘unbiasedness’ of  $M_s$  into  $M_s^*$ .* We call this method D&D++ (Fig. 2)

**Step 3 (D&D++):** Once  $M_s$  is trained, we initialize a new student network  $M_s^*$  using  $M_s$ .  $M_s^*$  is trained on the entire dataset with faces from both categories  $a_1$  and  $a_2$ , to improve its classification performance. During this, we use  $M_s$  as the teacher network and distill its ‘unbiasness’ to  $M_s^*$ . Here, we apply the same knowledge distillation used in step 2. We feed the training image to both  $M_s$  and  $M_s^*$  and obtain features  $f_s$  and  $f_s^*$  respectively.  $M_s$  remains frozen in this step. We use them to compute  $L_{dis}$  as:

$$L_{dis}(f_s, f_s^*) = 1 - \frac{f_s \cdot f_s^*}{\|f_s\| \|f_s^*\|}. \quad (6)$$

Combining  $L_{dis}$  with  $L_{class}$ , we train  $M_s^*$  with a bias reducing classification loss  $L_{br}$  defined as

$$L_{br} = L_{class} + \lambda_2 L_{dis}, \quad (7)$$

where  $\lambda_2$  is used to weight  $L_{dis}$  in D&D++. During inference, we use the trained  $M_s^*$  to perform verification.

## 5. Experiments

### 5.1. Network architectures and datasets

**Training dataset:** We use the BUPT-BalancedFace [56] dataset for training. For gender bias reduction, we create two subsets of this dataset: Male and female subset. We obtain the gender labels and perform face alignment in this dataset by using [46]. Each image in this dataset belongs to one of the four categories: African, Asian, Caucasian, Indian. Since there does not exist a large training dataset with skintone labels, we re-group this dataset according to skintone and build two subsets of the dataset on the basis of skintone for skintone bias reduction: Light (‘Caucasian’  $\cup$  ‘Asian’) and Dark (‘African’  $\cup$  ‘Indian’). Although skintone is not perfectly correlated with race, we elect to use these labels due to the high correlation with skintone.

**Evaluation dataset:** For evaluation, we use aligned faces from IJB-C, and follow the 1:1 face verification protocol from [37]. The alignment is done using [46]. This dataset provides gender and skintone labels. There are six classes for the skintone attribute which we reorganize into three groups, (i) *Light* (‘light pink’  $\cup$  ‘light yellow’), (ii) *Medium* (‘medium pink’  $\cup$  ‘medium yellow’), (iii) *Dark* (‘medium dark’  $\cup$  ‘dark brown’). For evaluating gender bias, we compute the face verification performance on male-male and female-female pairs separately (out of all the pairs defined in the IJB-C protocol [37]). For skintone bias, we compute the face verification performance on dark-dark and light-light pairs.

**Network architecture:** We implement the baselines and our proposed methods (D&D and D&D++) using Crystalface, proposed in [45], which is a Resnet-101 [28] network trained using crystal loss. To demonstrate the robustness of D&D and D&D++, we also perform similar experiments using Resnet50 [28] version of ArcFace [11].

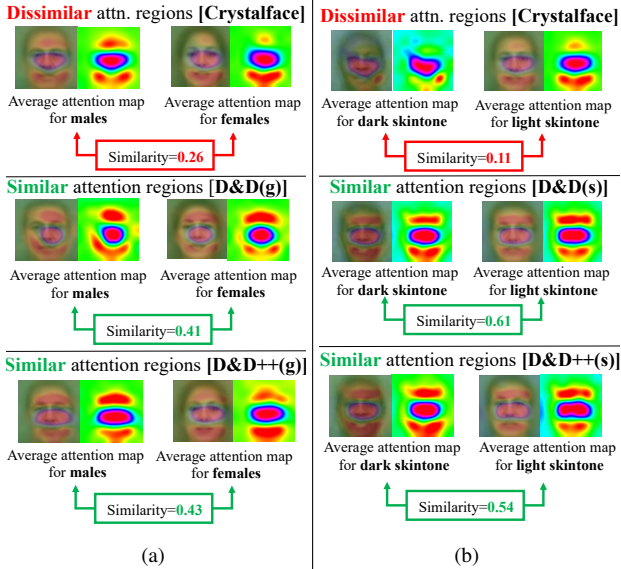


Figure 3. (a) D&D(g) and D&D++(g) generate more similar attention maps for male and female frontal faces, as compared to Crystalface. (b) D&D(s) and D&D++(s) generate more similar attention maps for dark and light frontal faces, than Crystalface.

## 5.2. D&D and D&D++ for gender and skintone

In Section 4.1, we present D&D and D&D++ as general approaches to reduce bias with respect to any binary attribute. Here, we show their usability to reduce gender and skintone bias (separately). We build two variants of our proposed frameworks: D&D(g) and D&D++(g) for reducing gender bias, and (ii) D&D(s) and D&D++(s) for reducing skintone bias. In D&D(g), the teacher  $M_t$  is trained on the female subset of the dataset, and student  $M_s$  (initialized with  $M_t$ ) is trained on the male images of the dataset (i.e. for  $A = \text{gender}$ ,  $a_1 = \text{Female}$  and  $a_2 = \text{Male}$ ). Similarly, in D&D(s), for  $A = \text{skintone}$ ,  $a_1 = \text{Light}$  and  $a_2 = \text{Dark}$ . For Step 3 in both D&D++(s) and D&D++(g), we train  $M_s^*$  on the entire BUPT-BalancedFace dataset, while performing feature-level distillation from  $M_s$ . In Sec. 5.4.1, we also perform experiments by reversing the sequence in which different attribute categories are learned. More training and hyperparameter ( $\lambda_1, \lambda_2$ ) details for D&D and D&D++ are provided in the supplementary material. The implementation code will be made publicly available upon publication.

## 5.3. Baseline methods

We compare our proposed methods with the following de-biasing methods. More training details and hyperparameter information for these baseline methods are provided in the supplementary material.

**PASS:** Protected Attribute Suppression System (PASS) [15] is a feature-based adversarial de-biasing framework, that has been proposed recently. Here, features are obtained from a pre-trained network  $P$  for the images in the

training dataset, and are adversarially made to reduce gender and race information. The authors present two PASS-based systems: PASS-g (for reducing gender information) and PASS-s (for reducing skintone information) in Crystalface features. Both PASS-g and PASS-s are built on top of features from the pre-trained Crystalface network  $P$ , which is trained on a combination of UMDFaces [7], UMDFaces-Videos [6] and MS1M [24] datasets. *But, UMDFaces [7] and UMDFaces-Videos [6] datasets are no longer publicly available<sup>1</sup>.* So, in our implementation, we train the network  $P$  on the publicly available BUPT-BalancedFace [56] dataset, after which we extract features for this dataset and perform adversarial training to reduce gender (PASS-g) and skintone information (PASS-s) in the extracted features. This also makes PASS systems comparable with our proposed methods: D&D and D&D++. We use the official implementation of PASS [14] for this task.

**Incremental Variable Elimination IVE** [55] is an attribute suppression algorithm that excludes variables in the face representation that affect attribute classification. Similar to [15], we use the official implementation of IVE [54] to construct two variants of IVE: IVE(g) and IVE(s) for gender and skintone bias mitigation, using features from Crystalface trained on the BUPT-BalancedFace dataset.

**Hair obscuring:** [1] show that obscuring hair in facial images during evaluation reduces gender bias by improving the similarity scores of genuine female-female pairs. We construct a similar pipeline to obscure hair for gender-bias mitigation by using face border keypoints computed by [46] for the images in the evaluation dataset (IJB-C). Following that, we extract features using Crystalface (trained on BUPT-BalancedFace) for all the images in the evaluation dataset and perform 1:1 verification.

**One step distillation (OSD)** The training sequence in D&D is  $M_t \rightarrow M_s$ , and for D&D++ is  $M_t \rightarrow M_s \rightarrow M_s^*$ , where  $M_s^*$  is trained on both attribute categories ( $a_1, a_2$ ). We construct a baseline called ‘One step distillation’ (OSD) for which the training sequence is  $M_t \rightarrow M_s^*$ . Here,  $M_t$  is trained on one attribute category ( $a_1$ ) and  $M_s^*$  (initialized with  $M_t$ ) is trained on both attribute categories ( $a_1, a_2$ ).  $M_s^*$  is constrained to mimic  $M_t$  through KD used in D&D and D&D++. We build two variants of OSD: OSD(g) for reducing gender bias and OSD(s) for reducing skintone bias. In OSD(g) we train  $M_t$  on female faces and  $M_s^*$  on both male and female faces. In OSD(s), we train  $M_t$  on light skintone faces and  $M_s^*$  on both dark and light faces.

## 5.4. Results with Crystalface

### 5.4.1 Effect on attention regions

We first select frontal facial images in IJB-C dataset for which the yaw angles (computed using [46]) lie between

<sup>1</sup><http://umdfaces.io/> Datasets unavailable

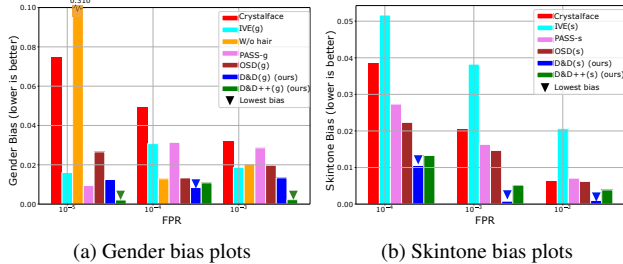


Figure 4. D&D or D&D++ obtain the lowest gender and skintone bias for Crystalface in IJB-C at all FPRs. Please see Sec. 5.3 for our implementation of baselines.

-5 to 5 degrees. We use GradCAM [52] to generate the attention maps for all of these images using the last convolutional layer of the Crystalface network. These attention maps highlight important face regions relevant for the face recognition decision. After that we separate out the attention maps for males and females, and average them separately. Figure 3a (first row) shows the average attention maps for males and females, generated using Crystalface.

**Similarity between male and female attention maps:** We compute the cosine similarity between the flattened average attention maps for males and females, which turns out to be low (0.26). This implies that male and female faces are processed differently by Crystalface. This might lead to gender bias, when features from Crystalface are used in face verification. Following this, we generate the average attention maps for males and females using Crystalface trained with D&D(g) and D&D++(g). From Fig. 3a (second and third row), it is clear that the male and female average attention maps are more similar when we use D&D(g) and D&D++(g), compared to Crystalface. This indicates that both male and female faces are processed in a more similar way with our distillation-based approaches.

**Similarity between light and dark attention maps:** We repeat this experiment to generate the average attention maps for frontal faces of light and dark skintone in IJB-C using Crystalface and its D&D(s) and D&D++(s) counterparts. Again, we find that the attention regions for dark and light faces generated using the original Crystalface network are dissimilar (cosine similarity=0.11), that might lead to skintone bias. However, the attention maps for light and dark skintones generated using D&D(s) and D&D++(s) are much more similar (Fig. 3b).

### 5.4.2 Evaluating gender and skintone bias

We now evaluate the effectiveness of D&D and D&D++ to reduce bias in terms of a given attribute. From Fig. 4, we infer that Crystalface networks trained with D&D/D&D++ obtain the lowest gender/skintone bias at most FPRs. This confirms our hypothesis (in Sec. 3), that networks that process faces belonging to different attribute categories in a similar way demonstrate lower attribute-bias. Also, from

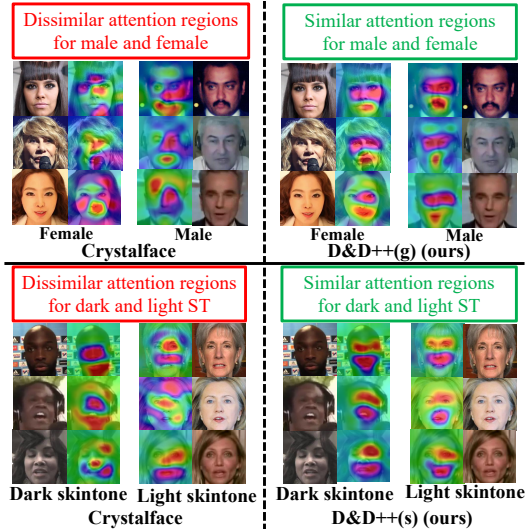


Figure 5. (Top) D&D++(g) attends to similar face regions for males and females. (Bottom) D&D++(s) attends to similar face regions for faces with dark and light skintones. The attention maps are generated using GradCAM [52]

Tables 2 and 3, we also infer that *D&D-based frameworks obtain higher BPCs (Eq. 3) than the baselines at all FPRs*. Moreover, it is clear that *D&D++ obtains better face verification performance than D&D and PASS [15]*, while maintaining low gender and skintone bias. This demonstrates the advantage of the additional step of training  $M_s^*$  on the full dataset, which adds specificity and transfers the ‘unbiasedness’ from  $M_s$  to  $M_s^*$  through distillation. We provide more qualitative results in Fig. 5 to show that D&D++ helps the network attend to similar spatial regions for both categories of the binary attribute under consideration. We provide the gender-wise, skintone-wise ROC plots (similar to the ROC curves in Fig. 1) in the supplementary material.

### 5.4.3 Reversing the order in D&D++

We also implement D&D++ by reversing the order in which attribute categories are used for training  $M_t$  and  $M_s$ . In D&D++(g), we train  $M_t$  with  $a_1 = \text{male (M)}$  and  $M_s$  (initialized with  $M_t$ ) with  $a_2 = \text{female (F)}$  (opposite to the sequence in Sec 5.2). Finally, we train a new student  $M_s^*$  on the entire dataset (‘All’). Comparing the top row of Table A4 with Table 2, it is clear that even with this sequence (i.e.  $M \rightarrow F \rightarrow \text{‘All’}$ ), D&D++(g) obtains higher  $BPC_g$  and lower gender bias than baselines. Repeating this experiment for D&D++(s), we train  $M_t$  with  $a_1 = \text{dark (D)}$  and  $M_s$  with  $a_2 = \text{light (L)}$  (opposite to the sequence in Sec 5.2). Table A4 (bottom row) shows that D&D++(s) trained with this sequence also obtains lower skintone bias and higher  $BPC_{st}$  than baselines at most FPRs. Thus, we can train D&D++(g/s) with any sequence of attribute categories to lower gender/skintone bias, while maintaining reasonable face verification performance.

FPR	10 <sup>-5</sup>					10 <sup>-4</sup>					10 <sup>-3</sup>				
	Method	TPR	TPR <sub>m</sub>	TPR <sub>f</sub>	Bias(↓)	BPC <sub>g</sub> (↑)	TPR	TPR <sub>m</sub>	TPR <sub>f</sub>	Bias(↓)	BPC <sub>g</sub> (↑)	TPR	TPR <sub>m</sub>	TPR <sub>f</sub>	Bias(↓)
Crystalface	0.856	0.869	0.794	0.075	0	0.912	0.920	0.871	0.049	0	0.950	0.953	0.921	0.031	0
IVE(g) <sup>†</sup> [55]	0.840	0.820	0.804	0.016	<u>0.768</u>	0.910	0.911	0.880	0.031	0.365	0.952	0.951	0.932	0.019	0.389
W/o hair <sup>†</sup> [1]	0.592	0.396	0.706	0.310	-3.441	0.803	0.770	0.783	0.013	0.615	0.899	0.888	0.868	0.020	0.301
PASS-g <sup>†</sup> [15]	0.691	0.656	0.647	<u>0.009</u>	0.687	0.842	0.832	0.800	0.031	0.291	0.914	0.918	0.890	0.029	0.027
OSD(g)	0.721	0.712	0.738	0.027	0.482	0.817	0.815	0.828	0.013	0.631	0.895	0.888	0.908	0.020	0.297
D&D(g)	0.705	0.693	0.706	0.013	0.650	0.805	0.805	0.813	<b>0.008</b>	<b>0.719</b>	0.888	0.883	0.896	<u>0.013</u>	<u>0.515</u>
D&D++(g)	0.754	0.744	0.741	<b>0.002</b>	<b>0.854</b>	0.844	0.841	0.830	<u>0.011</u>	<u>0.701</u>	0.914	0.910	0.907	<b>0.002</b>	<b>0.898</b>

Table 2. *Gender bias analysis for Crystalface network, and its de-biased counterparts on IJB-C. TPR: overall True Positive rate, TPR<sub>m</sub>: male-male TPR, TPR<sub>f</sub>: female-female TPR. **Bold**=Best, Underlined=Second best. D&D variants obtain higher BPC<sub>g</sub> and lower gender bias at most FPRs. <sup>†</sup>=Our implementation of baselines (See 5.3 for details). All methods are trained on BUPT-BalancedFace [56] data.*

FPR	10 <sup>-4</sup>					10 <sup>-3</sup>					10 <sup>-2</sup>				
	Method	TPR	TPR <sub>l</sub>	TPR <sub>d</sub>	Bias(↓)	BPC <sub>st</sub> (↑)	TPR	TPR <sub>l</sub>	TPR <sub>d</sub>	Bias(↓)	BPC <sub>st</sub> (↑)	TPR	TPR <sub>l</sub>	TPR <sub>d</sub>	Bias(↓)
Crystalface	0.912	0.906	0.867	0.038	0	0.950	0.945	0.925	0.020	0	0.973	0.970	0.963	0.006	0
IVE(s) <sup>†</sup> [55]	0.910	0.906	0.854	0.072	-0.371	0.950	0.948	0.909	0.038	-0.900	0.974	0.974	0.953	0.021	-2.49
PASS-s <sup>†</sup> [15]	0.851	0.842	0.815	0.027	0.222	0.910	0.903	0.886	0.016	0.158	0.953	0.953	0.946	0.007	-0.187
OSD(s)	0.848	0.819	0.841	0.022	0.351	0.916	0.899	0.913	0.015	0.214	0.961	0.953	0.959	0.006	-0.012
D&D(s)	0.850	0.828	0.839	<b>0.011</b>	<b>0.643</b>	0.916	0.903	0.904	<b>0.001</b>	<b>0.914</b>	0.961	0.953	0.952	<b>0.001</b>	<b>0.821</b>
D&D++(s)	0.886	0.875	0.862	<u>0.013</u>	<u>0.629</u>	0.934	0.926	0.921	<u>0.005</u>	<u>0.733</u>	0.967	0.963	0.959	<u>0.004</u>	<u>0.327</u>

Table 3. *Skintone bias analysis for Crystalface network, and its de-biased counterparts on IJB-C. TPR<sub>l</sub>: light-light TPR, TPR<sub>d</sub>: dark-dark TPR. **Bold**=Best, Underlined=Second best. D&D variants obtain higher BPC<sub>st</sub> and lower skintone bias at most FPRs. <sup>†</sup>=Our implementation of baselines (Refer to Sec. 5.3 for details). All the methods are trained on BUPT-BalancedFace [56] dataset.*

FPR	10 <sup>-5</sup>		10 <sup>-4</sup>		10 <sup>-3</sup>	
	Sequence	Bias(↓) BPC <sub>g</sub> (↑)				
F→M→All	0.002	<b>0.854</b>	0.011	0.701	0.002	0.898
M→F→All	0.024	0.501	0.004	<b>0.809</b>	0	<b>0.940</b>
FPR	10 <sup>-4</sup>		10 <sup>-3</sup>		10 <sup>-2</sup>	
	Sequence	Bias(↓) BPC <sub>st</sub> (↑)				
L→D→All	0.013	<b>0.629</b>	0.005	<b>0.733</b>	0.004	<b>0.327</b>
D→L→All	0.012	0.615	0.010	0.461	0.006	-0.023

Table 4. Reversing the order in which different genders/skintones are learned in (**top**) D&D++(g) and (**bottom**) D&D++(s). Here, L=light and D=dark skintone subset of BUPTBalancedFace. F=female and M=male subset of the dataset. ‘All’=entire dataset. *Detailed results including attention regions are provided in the supplementary material.*

FPR	10 <sup>-5</sup>		10 <sup>-4</sup>		10 <sup>-3</sup>	
	Method	TPR	BPC <sub>g</sub> (↑)	TPR	BPC <sub>g</sub> (↑)	TPR
ArcFace	0.879	0.00	0.914	0.00	0.944	0
IVE(g) <sup>†</sup> [55]	0.877	0.021	0.913	-0.064	0.944	0
W/o hair <sup>†</sup> [1]	0.726	-8.91	0.883	-1.97	0.926	<u>0.746</u>
PASS-g <sup>†</sup> [15]	0.798	-1.162	0.869	<u>0.607</u>	0.909	0.198
OSD(g)	0.778	0.361	0.848	0.397	0.898	0.010
D&D(g)	0.759	<u>0.483</u>	0.830	0.596	0.889	0.412
D&D++(g)	0.825	<b>0.891</b>	0.880	<b>0.682</b>	0.920	<b>0.857</b>

Table 5. *Gender bias analysis for ArcFace network, and its de-biased counterparts on IJB-C. **Bold**=Best, Underlined=Second best. D&D variants obtain highest BPC<sub>g</sub> at most FPRs. <sup>†</sup>=Our implementation of baselines (Refer to Sec. 5.5 for details). All the methods are trained on BUPT-BalancedFace [56] dataset.*

FPR	10 <sup>-4</sup>		10 <sup>-3</sup>		10 <sup>-2</sup>	
	Method	TPR	BPC <sub>st</sub> (↑)	TPR	BPC <sub>st</sub> (↑)	TPR
ArcFace	0.914	0	0.944	0	0.964	0
IVE(s) <sup>†</sup> [55]	0.913	-0.380	0.943	-0.049	0.964	0.214
PASS-s <sup>†</sup> [15]	0.786	-0.554	0.861	0.245	0.920	<b>0.883</b>
OSD(s)	0.877	<u>0.787</u>	0.923	0.216	0.956	0.349
D&D(s)	0.855	0.418	0.913	<u>0.443</u>	0.951	0.629
D&D++(s)	0.882	<b>0.862</b>	0.926	<b>0.457</b>	0.957	<u>0.778</u>

Table 6. *Skintone bias analysis for ArcFace network, and its de-biased counterparts on IJB-C. **Bold**=Best, Underlined=Second best. D&D variants obtain higher BPC<sub>st</sub> at most FPRs. <sup>†</sup>=Our implementation of baselines (Refer to Sec. 5.5 for details). All the methods are trained on BUPT-BalancedFace [56] dataset.*

## 5.5. Results with Arcface

We repeat the aforementioned experiments on the ResNet-50 version of ArcFace [11]. Fig. 6 shows that *D&D and D&D++ generate more similar attention maps for male and female faces (and for faces with dark and light skintone)*, than the original Arcface network. We also implement the gender-debiasing baselines (Hair obscuring, IVE(g), PASS-g) and skintone-debiasing baselines (IVE(s), PASS-s) using the ResNet-50 backbone of Arcface to make fair comparison with D&D-based methods. *ArcFace networks trained with D&D/D&D++ obtain the lowest gender and skintone bias (Fig. 7), and highest BPC scores (Tables A5, A6)*. Also, D&D++ achieves considerably higher TPR than D&D (Tables A5, A6). The hyperparameter information and detailed results (including ROC curves) for all the methods are provided in the supplementary material.

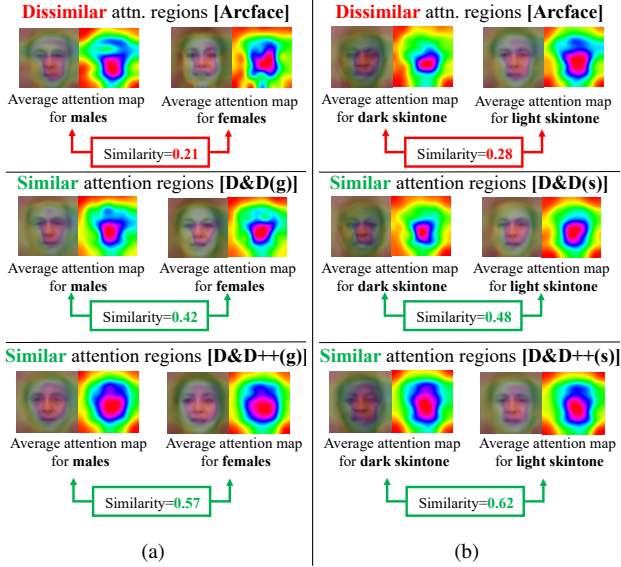


Figure 6. (a) D&D(g) and D&D++(g) generate more similar attention maps for male and female frontal faces, as compared to Arcface. (b) D&D(s) and D&D++(s) generate more similar attention maps for dark and light frontal faces, than Arcface.

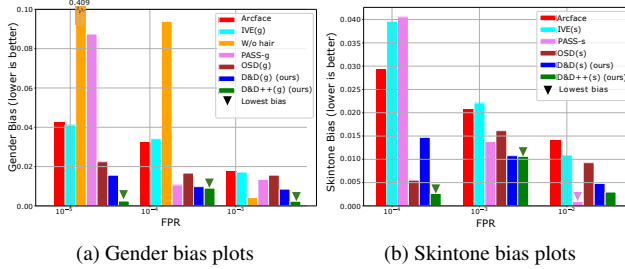


Figure 7. D&D or D&D++ obtain the lowest gender and skintone bias for ArcFace in IJB-C at most FPRs. Please see Sec. 5.5 and supplementary material for our implementation of baselines.

## 5.6. Bias v/s face verification performance

Although an ideal de-biasing system would reduce bias while maintaining face verification performance, existing adversarial de-biasing algorithms such as PASS [15], Deb-Face [21], AGENDA [17] etc. demonstrate significant drop in face verification performance. In this work, we provide insights for reducing bias while minimizing the drop in face verification performance by presenting D&D++, which is a non-adversarial approach. We recognize that D&D++(s/g) also demonstrates drop in face verification performance. This drop may be caused by the explicit distillation constraint ( $L_{dis}$ ) imposed on the D&D++ student  $M_s^*$  that restricts  $M_s^*$  from learning all the gender or skintone specific details. However, compared to de-biasing methods such as PASS [15] that explicitly remove protected attributes from face representations, the drop in verification performance with D&D++ is considerably lower (Fig. 8). For instance, in Table A5, the drop in verification TPR@FPR=10<sup>-5</sup> is 5.4% with D&D++(g), as compared to the original Arcface

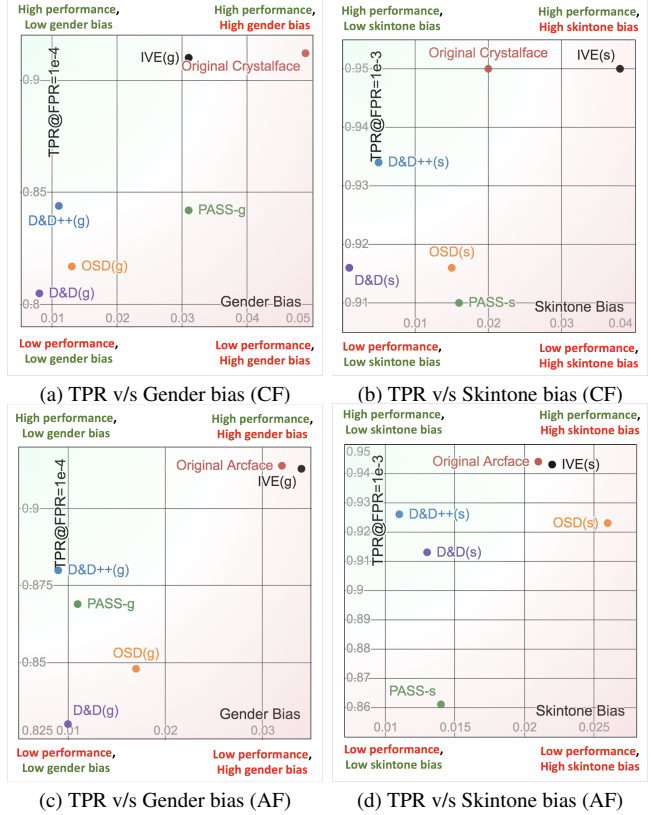


Figure 8. TPR at a fixed FPR v/s Gender/Skintone bias demonstrated by de-biasing methods based on (a,b) Crystalface (CF) and (c,d) ArcFace (AF). Ideally, a de-biasing method would occupy the upper-left-hand corner, where performance is high, and bias is low (mostly occupied by D&D++). The lower right-hand is the worst case which decreases performance without reducing bias.

network. With PASS-g, this drop is 8.1%. Similar trends can be found in Tables 2, 3, A6 at most FPRs. Hence, we believe that non-adversarial methods like D&D++ are more practical for reducing bias, since adversarial methods significantly lower the identity classifying capability of a network by removing sensitive attributes to achieve ‘fairness through blindness’.

## 6. Conclusion

We present two novel knowledge distillation-based techniques (D&D and D&D++) to incrementally learn different categories of an attribute. We observe that our proposed methods enforce the networks to attend to similar spatial regions of the face for both categories of an attribute and consequently reduce bias w.r.t. that attribute. We show the effectiveness of these methods to reduce bias w.r.t. two attributes: gender and skintone. Both D&D and D&D++ outperform the existing baselines in reducing bias. D&D++, while being less biased than baselines, generally obtains better face verification performance than SOTA adversarial de-biasing algorithms. We also show the generalizability of our methods on two SOTA face recognition networks.

## Acknowledgement

This research is based upon work supported by a MURI from the Army Research Office under the Grant No. W911NF-17-1-0304. This is part of the collaboration between US DOD, UK MOD and UK Engineering and Physical Research Council (EPSRC) under the Multidisciplinary University Research Initiative. Carlos D. Castillo was supported by funding provided by National Eye Institute Grant R01EY029692-03.

## References

- [1] V Albiero and KW Bowyer. Is face recognition sexist? no, gendered hairstyles and biology are. *BMVC 2020*, 2020. [2](#), [5](#), [7](#), [11](#), [16](#), [19](#)
- [2] V Albiero, KS Krishnapriya, K Vangara, K Zhang, MC King, and KW Bowyer. Analysis of gender inequality in face recognition accuracy. In *Proceedings of the IEEE Winter Conference on Applications of Computer Vision Workshops*, pages 81–89, 2020. [2](#)
- [3] V Albiero, K Zhang, and KW Bowyer. How does gender balance in training data affect face recognition accuracy? *2020 IEEE International Joint Conference on Biometrics (IJCB)*, 2020. [1](#), [2](#)
- [4] M Alvi, A Zisserman, and C Nellåker. Turning a blind eye: Explicit removal of biases and variation from deep neural network embeddings. In *Proceedings of the European Conference on Computer Vision (ECCV) Workshops*, pages 0–0, 2018. [2](#)
- [5] A Amini, AP Soleimany, W Schwarting, SN Bhatia, and D Rus. Uncovering and mitigating algorithmic bias through learned latent structure. In *Proceedings of the 2019 AAAI/ACM Conference on AI, Ethics, and Society*, pages 289–295, 2019. [1](#), [2](#)
- [6] A Bansal, CD Castillo, R Ranjan, and R Chellappa. The do’s and don’ts for CNN-based face verification. In *Proceedings of the IEEE International Conference on Computer Vision*, pages 2545–2554, 2017. [5](#), [17](#)
- [7] A Bansal, A Nanduri, C D Castillo, R Ranjan, and R Chellappa. Umdfaces: An annotated face dataset for training deep networks. In *2017 IEEE International Joint Conference on Biometrics (IJCB)*, pages 464–473. IEEE, 2017. [5](#), [17](#)
- [8] J Buolamwini and T Gebru. Gender shades: Intersectional accuracy disparities in commercial gender classification. In *Conference on fairness, accountability and transparency*, pages 77–91, 2018. [2](#)
- [9] Jacqueline G. Cavazos, P. Jonathon Phillips, Carlos D. Castillo, and Alice J. O’Toole. Accuracy comparison across face recognition algorithms: Where are we on measuring race bias? *IEEE transactions on biometrics, behavior, and identity science*, 3:101–111, 2021. [1](#)
- [10] CM Cook, JJ Howard, YB Sirotin, and JL Tipton. Fixed and varying effects of demographic factors on the performance of eleven commercial facial recognition systems. *IEEE Transactions on Biometrics, Behavior, and Identity Science*, 40(1), 2019. [2](#)
- [11] J Deng, J Guo, X Niannan, and S Zafeiriou. Arcface: Additive angular margin loss for deep face recognition. In *CVPR*, 2019. [1](#), [2](#), [4](#), [7](#), [14](#)
- [12] P Dhar, A Bansal, CD Castillo, J Gleason, PJ Phillips, and R Chellappa. How are attributes expressed in face dcnn’s? In *2020 15th IEEE International Conference on Automatic Face and Gesture Recognition (FG 2020)*, pages 85–92. IEEE, 2020. [2](#)
- [13] P Dhar, C Castillo, and R Chellappa. On measuring the iconicity of a face. In *2019 IEEE Winter Conference on Applications of Computer Vision (WACV)*, pages 2137–2145. IEEE, 2019. [1](#)
- [14] Prithviraj Dhar, Joshua Gleason, Aniket Roy, Carlos D. Castillo, and Rama Chellappa. PASS codebase. <https://github.com/Prithviraj7/PASS>, 2021. [5](#), [11](#), [16](#), [18](#)
- [15] Prithviraj Dhar, Joshua Gleason, Aniket Roy, Carlos D. Castillo, and Rama Chellappa. PASS: Protected Attribute Suppression System for Mitigating Bias in Face Recognition. In *Proceedings of the IEEE/CVF International Conference on Computer Vision (ICCV)*, pages 15087–15096, October 2021. [1](#), [2](#), [3](#), [5](#), [6](#), [7](#), [8](#), [11](#), [13](#), [15](#), [16](#), [17](#), [18](#), [19](#)
- [16] Prithviraj Dhar, Joshua Gleason, Hossein Souri, Carlos D Castillo, and Rama Chellappa. An adversarial learning algorithm for mitigating gender bias in face recognition. *arXiv e-prints*, pages arXiv–2006, 2020. [1](#)
- [17] Prithviraj Dhar, Joshua Gleason, Hossein Souri, Carlos D Castillo, and Rama Chellappa. Towards gender-neutral face descriptors for mitigating bias in face recognition. *arXiv preprint arXiv:2006.07845*, 2020. [8](#)
- [18] Prithviraj Dhar, Rajat Vikram Singh, Kuan-Chuan Peng, Ziyang Wu, and Rama Chellappa. Learning without memorizing. In *Proceedings of the IEEE/CVF Conference on Computer Vision and Pattern Recognition*, pages 5138–5146, 2019. [2](#)
- [19] Pawel Drozdowski, Christian Rathgeb, Antitza Dantcheva, Naser Damer, and Christoph Busch. Demographic bias in biometrics: A survey on an emerging challenge. *IEEE Transactions on Technology and Society*, 1(2):89–103, 2020. [2](#)
- [20] Thomas B Fitzpatrick. Soleil et peau. *J Med Esthet*, 2:33–34, 1975. [2](#)
- [21] S Gong, X Liu, and AK Jain. Jointly de-biasing face recognition and demographic attribute estimation. In *European Conference on Computer Vision*, pages 330–347. Springer, 2020. [1](#), [2](#), [8](#), [15](#), [16](#), [18](#)
- [22] S Gong, X Liu, and AK Jain. Mitigating face recognition bias via group adaptive classifier. In *In Proceeding of IEEE Computer Vision and Pattern Recognition*, Nashville, TN, June 2021. [2](#), [18](#)
- [23] Patrick Grother, Mei Ngan, and Kayee Hanaoka. *Face Recognition Vendor Test (FVRT): Part 3, Demographic Effects*. National Institute of Standards and Technology, 2019. [1](#), [2](#)
- [24] Y. Guo, L. Zhang, Y. Hu, X. He, and J. Gao. Ms-celeb-1m: A dataset and benchmark for large-scale face recognition. In *European Conference on Computer Vision*, pages 87–102. Springer, 2016. [5](#), [15](#), [17](#)

- [25] Moritz Hardt, Eric Price, and Nati Srebro. Equality of opportunity in supervised learning. In *NIPS*, 2016. 11
- [26] Caner Hazirbas, Joanna Bitton, Brian Dolhansky, Jacqueline Pan, Albert Gordo, and Cristian Canton Ferrer. Casual conversations: A dataset for measuring fairness in ai. In *Proceedings of the IEEE/CVF Conference on Computer Vision and Pattern Recognition*, pages 2289–2293, 2021. 2
- [27] K. He, X. Zhang, S. Ren, and J. Sun. Deep residual learning for image recognition. *arXiv preprint arXiv:1512.03385*, 2015. 16
- [28] K. He, X. Zhang, S. Ren, and J. Sun. Deep residual learning for image recognition. In *IEEE Conference on Computer Vision and Pattern Recognition (CVPR)*, pages 770–778, 2016. 4
- [29] MQ Hill, CJ Parde, CD Castillo, YI Colon, R Ranjan, JC Chen, V Blanz, and AJ O’Toole. Deep convolutional neural networks in the face of caricature. *Nature Machine Intelligence*, 1(11):522–529, 2019. 2
- [30] Geoffrey Hinton, Oriol Vinyals, and Jeffrey Dean. Distilling the knowledge in a neural network. In *NIPS Deep Learning and Representation Learning Workshop*, 2015. 2
- [31] BF Klare, MJ Burge, JC Klontz, RWV Bruegge, and AK Jain. Face recognition performance: Role of demographic information. *IEEE Transactions on Information Forensics and Security*, 7(6):1789–1801, 2012. 2
- [32] KS Krishnapriya, Vitor Albiero, Kushal Vangara, Michael C King, and Kevin W Bowyer. Issues related to face recognition accuracy varying based on race and skin tone. *IEEE Transactions on Technology and Society*, 1(1):8–20, 2020. 1
- [33] K. S Krishnapriya, Kushal Vangara, Michael C King, Vitor Albiero, and Kevin Bowyer. Characterizing the variability in face recognition accuracy relative to race. In *Proceedings of the IEEE Conference on Computer Vision and Pattern Recognition Workshops*, pages 0–0, 2019. 1
- [34] A Li, J Guo, H Yang, and Y Chen. Deepobfuscator: Adversarial training framework for privacy-preserving image classification. *arXiv preprint arXiv:1909.04126*, 2019. 2
- [35] Zhizhong Li and Derek Hoiem. Learning without forgetting. *IEEE transactions on pattern analysis and machine intelligence*, 40(12):2935–2947, 2017. 2, 4
- [36] B Lu, JC Chen, CD Castillo, and R Chellappa. An experimental evaluation of covariates effects on unconstrained face verification. *IEEE Transactions on Biometrics, Behavior, and Identity Science*, 1(1):42–55, 2019. 2
- [37] B Maze, J Adams, J A Duncan, N Kalka, T Miller, C Otto, A K Jain, W T Niggel, J Anderson, J Cheney, et al. IARPA janus benchmark-c: Face dataset and protocol. In *2018 International Conference on Biometrics (ICB)*, pages 158–165. IEEE, 2018. 2, 4, 13, 15
- [38] Qiang Meng, Shichao Zhao, Zhida Huang, and Feng Zhou. MagFace: A universal representation for face recognition and quality assessment. In *CVPR*, 2021. 1
- [39] Shruti Nagpal, Maneet Singh, Richa Singh, and Mayank Vatsa. Diversity blocks for de-biasing classification models. In *2020 IEEE International Joint Conference on Biometrics (IJCB)*, pages 1–9. IEEE, 2020. 2
- [40] Shruti Nagpal, Maneet Singh, Richa Singh, Mayank Vatsa, and Nalini Ratha. Deep learning for face recognition: Pride or prejudiced? *arXiv preprint arXiv:1904.01219*, 2019. 1
- [41] Sungho Park, Sunhee Hwang, Dohyung Kim, and Hyeran Byun. Learning disentangled representation for fair facial attribute classification via fairness-aware information alignment. In *Proceedings of the AAAI Conference on Artificial Intelligence*, volume 35, pages 2403–2411, 2021. 2
- [42] PJ Phillips, PJ Flynn, T Scruggs, KW Bowyer, J Chang, K Hoffman, J Marques, J Min, and W Worek. Overview of the face recognition grand challenge. In *2005 IEEE computer society conference on computer vision and pattern recognition (CVPR’05)*, volume 1, pages 947–954. IEEE, 2005. 19
- [43] P Jonathon Phillips, Fang Jiang, Abhijit Narvekar, Julianne Ayyad, and Alice J O’Toole. An other-race effect for face recognition algorithms. *ACM Transactions on Applied Perception (TAP)*, 8(2):14, 2011. 1
- [44] Andraž Puc, Vitomir Štruc, and Klemen Grm. Analysis of race and gender bias in deep age estimation models. In *2020 28th European Signal Processing Conference (EUSIPCO)*, pages 830–834. IEEE, 2021. 2
- [45] R Ranjan, A Bansal, J Zheng, H Xu, J Gleason, B Lu, A Nanduri, J-C Chen, C D Castillo, and R Chellappa. A fast and accurate system for face detection, identification, and verification. *IEEE Transactions on Biometrics, Behavior, and Identity Science*, 1(2):82–96, 2019. 1, 2, 4
- [46] R Ranjan, S Sankaranarayanan, C D Castillo, and R Chellappa. An all-in-one convolutional neural network for face analysis. In *2017 12th IEEE International Conference on Automatic Face & Gesture Recognition (FG 2017)*, pages 17–24. IEEE, 2017. 4, 5, 19
- [47] Sylvestre-Alvise Rebuffi, Alexander Kolesnikov, Georg Sperl, and Christoph H Lampert. iCaRL: Incremental classifier and representation learning. In *Proc. CVPR*, 2017. 2
- [48] K Ricanek and T Tesafaye. Morph: A longitudinal image database of normal adult age-progression. In *7th International Conference on Automatic Face and Gesture Recognition (FGR06)*, pages 341–345. IEEE, 2006. 19
- [49] JP Robinson, G Livitz, Y Henon, C Qin, Y Fu, and S Timoner. Face recognition: too bias, or not too bias? In *Proceedings of the IEEE/CVF Conference on Computer Vision and Pattern Recognition Workshops*, pages 0–1, 2020. 2
- [50] Joseph P Robinson, Can Qin, Yann Henon, Samson Timoner, and Yun Fu. Balancing biases and preserving privacy on balanced faces in the wild. *arXiv preprint arXiv:2103.09118*, 2021. 2
- [51] Adriana Romero, Nicolas Ballas, Samira Ebrahimi Kahou, Antoine Chassang, Carlo Gatta, and Yoshua Bengio. Fitnets: Hints for thin deep nets. *ICLR 2015*, 2015. 2, 4
- [52] R R Selvaraju, M Cogswell, A Das, R Vedantam, D Parikh, and D Batra. Grad-cam: Visual explanations from deep networks via gradient-based localization. In *Proceedings of the IEEE International Conference on Computer Vision*, pages 618–626, 2017. 2, 6
- [53] Y Taigman, M Yang, M Ranzato, and L Wolf. Deepface: Closing the gap to human-level performance in face verification. In *Proceedings of the IEEE Conference on Computer Vision and Pattern Recognition*, pages 1701–1708, 2014. 1

- [54] P Terhörst, N Damer, F Kirchbuchner, and A Kuijper. IVE codebase. [https://github.com/pterhoer/PrivacyPreservingFaceRecognition/tree/master/supervised/incremental\\_variable\\_elimination](https://github.com/pterhoer/PrivacyPreservingFaceRecognition/tree/master/supervised/incremental_variable_elimination), 2019. 5, 11, 19
- [55] P Terhörst, N Damer, F Kirchbuchner, and A Kuijper. Suppressing gender and age in face templates using incremental variable elimination. In *2019 International Conference on Biometrics (ICB)*, pages 1–8. IEEE, 2019. 5, 7, 15, 16, 18, 19
- [56] M Wang and W Deng. Mitigating bias in face recognition using skewness-aware reinforcement learning. In *Proceedings of the IEEE/CVF Conference on Computer Vision and Pattern Recognition*, pages 9322–9331, 2020. 2, 4, 5, 7, 13, 15, 16, 17
- [57] M Wang, W Deng, J Hu, X Tao, and Y Huang. Racial faces in the wild: Reducing racial bias by information maximization adaptation network. In *Proceedings of the IEEE International Conference on Computer Vision*, pages 692–702, 2019. 1, 2
- [58] T Wang, J Zhao, M Yatskar, KW Chang, and V Ordonez. Balanced datasets are not enough: Estimating and mitigating gender bias in deep image representations. In *Proceedings of the IEEE International Conference on Computer Vision*, pages 5310–5319, 2019. 1
- [59] Tian Xu, Jennifer White, Sinan Kalkan, and Hatice Gunes. Investigating bias and fairness in facial expression recognition. In *European Conference on Computer Vision*, pages 506–523. Springer, 2020. 2
- [60] Xingkun Xu, Yuge Huang, Pengcheng Shen, Shaoxin Li, Jilin Li, Feiyue Huang, Yong Li, and Zhen Cui. Consistent instance false positive improves fairness in face recognition. In *Proceedings of the IEEE/CVF Conference on Computer Vision and Pattern Recognition*, pages 578–586, 2021. 13
- [61] Zhanjia Yang, Xiangping Zhu, Changyuan Jiang, Wenshuang Liu, and Linlin Shen. Ramface: Race adaptive margin based face recognition for racial bias mitigation. In *2021 IEEE International Joint Conference on Biometrics (IJCB)*, pages 1–8. IEEE, 2021. 2
- [62] C Yu, J Wang, C Peng, C Gao, G Yu, and N Sang. Bisenet: Bilateral segmentation network for real-time semantic segmentation. In *Proceedings of the European conference on computer vision (ECCV)*, pages 325–341, 2018. 19
- [63] Sergey Zagoruyko and Nikos Komodakis. Paying more attention to attention: Improving the performance of convolutional neural networks via attention transfer. In *ICLR*, 2017. 2

## Supplementary material

In this supplementary material, we provide the following information:

**Section A1:** A novel interpretation of the bias measure (introduced in [15]) as a metric for Equality of Odds.

**Section A2:** Training details for OSD, D&D, and D&D++.

**Section A3:** Detailed results with Crystalface (Section A3.1) and Arcface (Section A3.2) backbones, including verification ROCs and qualitative results. We also provide the

Table/Fig.	Summary
Table A2	Hyperparameters for D&D, D&D++, OSD
Fig. A1	Gender & Skintone-wise verification plots for Crystalface and its debiasing counterparts
Fig. A2	Overall verification plots for Crystalface and its debiasing counterparts
Fig. A3	Qualitative results for Crystalface-based D&D++
Table A4	Extension of <b>Table 4</b> from the main paper
Fig. A4	Gender and skintone wise verification plots with D&D++ and reverse-ordered D&D++
Fig. A5	Avg. attention maps for D&D++ and reverse-ordered D&D++
Fig. A8	Gender & Skintone-wise verification plots for Arcface and its debiasing counterparts
Fig. A9	Overall verification plots for Arcface and its debiasing counterparts
Table A5	Gender bias analysis with Arcface-based methods (Extension of <b>Table 5</b> from the main paper)
Table A6	Skintone bias analysis with Arcface-based methods (Extension of <b>Table 6</b> from the main paper)
Fig. A7	Qualitative results for Arcface-based D&D++
Fig. A10	Extension of <b>Fig. 8</b> from the main paper
Table A8	Hyperparameters for PASS

Table A1. **Summary of main results:** For the readers’ convenience, we provide a brief summary of the important results in this supplementary material.

plots for TPR at a fixed FPR v/s Gender/Skintone bias in Section A3.3

**Section A4:** Training details for PASS [15] baselines, following the official implementation [14].

**Section A5:** Training details for IVE, following the official implementation [54].

**Section A6:** Pipeline for obscuring hair (similar to [1]).

A brief summary of the main results in this supplementary material is provided in **Table A1**.

## A1. Zero Bias implies Equality of Odds

We use the bias measures introduced in previous bias mitigation work [15]. Here, we show that it may be viewed as a measure of *equality of odds* [25] for pair-wise matching in the sense that achieving zero bias (as defined in Eq A1) allows us to achieve equality of odds.

First, we define bias at a false positive rate (FPR) of  $F$

with respect to attribute  $A$  as

$$\text{Bias}^{(F)} = |\text{TPR}_{a_0}^{(F)} - \text{TPR}_{a_1}^{(F)}|, \quad (\text{A1})$$

where  $\text{TPR}_{a_*}^{(F)}$  denotes the true positive rate (TPR) on pairs of faces with attribute  $A = a_*$  at FPR of  $F$ .

Next, we show how achieving zero bias in equation A1 satisfies equalized odds. First let  $\mathcal{F}$  be the set of all face images and let  $A : \mathcal{F} \rightarrow \{0, 1\}$  be an indicator on a binary attribute of a face where 0 corresponds to  $a_0$  and 1 corresponds to  $a_1$ . Let  $\Omega_A \equiv \{(f_1, f_2) \in \mathcal{F} \times \mathcal{F} \mid A(f_1) = A(f_2)\}$  be the set of all pairs of faces with matching attributes and let  $Y : \Omega_A \rightarrow \{0, 1\}$  indicate identity equivalence for a pair of faces. Since all pairs in  $\Omega_A$  consist of faces with equal values of  $A$  we extend  $A$  onto  $\Omega_A$  such that  $A(f_1, f_2) = A(f_1)$  for all  $(f_1, f_2) \in \Omega_A$ . Finally, let  $\hat{Y} : \Omega_A \rightarrow \{0, 1\}$  be a predictor of  $Y$ . Supposing  $\omega \in \Omega_A$  is random pair of faces sampled from  $\Omega_A$ , then we have *equality of odds* if and only if

$$\begin{aligned} P(\hat{Y}(\omega) = 1 \mid A(\omega) = 0, Y(\omega) = 1) = \\ P(\hat{Y}(\omega) = 1 \mid A(\omega) = 1, Y(\omega) = 1) \end{aligned} \quad (\text{A2})$$

and

$$\begin{aligned} P(\hat{Y}(\omega) = 1 \mid A(\omega) = 0, Y(\omega) = 0) = \\ P(\hat{Y}(\omega) = 1 \mid A(\omega) = 1, Y(\omega) = 0). \end{aligned} \quad (\text{A3})$$

Equation A2 is equivalent to  $\text{TPR}_{a_0}^{(F)} = \text{TPR}_{a_1}^{(F)}$  for a fixed FPR of  $F$ , while equation A3 corresponds to a equal FPR for both  $a_0$  and  $a_1$  pairs.

Equation A2 is clearly satisfied when the bias measure in equation A1 is zero. Equation A3 is satisfied by selecting two appropriate thresholds, one for pairs with attribute  $A = a_0$  and another for pairs with attribute  $A = a_1$ . In this way, we have shown that minimizing the bias term defined in equation A1 works towards achieving equalized odds in pair-wise face matching.

## A2. Training details for D&D, D&D++ and OSD

### A2.1. D&D and D&D++

In Section 4.2 of the main paper, we explain the D&D and D&D++ approaches in detail. We define a bias reducing classification loss  $L_{br}$  to train the student network  $M_s$  in step 2 as

$$L_{br} = L_{class} + \lambda_1 L_{dis}, \quad (\text{A4})$$

where  $\lambda_1$  is used to weight  $L_{dis}$  in D&D. Once  $M_s$  is trained, we add another step (step 3) called D&D++ and initialize a new student network  $M_s^*$  with  $M_s$  and train it on both categories of the binary attribute  $A$ . During this phase,

Method/Backbone	Crystalface	ArcFace
OSD(g)	$\lambda_{osd} = 0.8$	$\lambda_{osd} = 1.0$
D&D(g)	$\lambda_1 = 1.0$	$\lambda_1 = 1.0$
D&D++(g)	$\lambda_2 = 1.0$	$\lambda_2 = 1.0$
OSD(s)	$\lambda_{osd} = 0.3$	$\lambda_{osd} = 0.5$
D&D(s)	$\lambda_1 = 0.5$	$\lambda_1 = 1.0$
D&D++(s)	$\lambda_2 = 0.5$	$\lambda_2 = 1.0$

Table A2. Hyperparameters for training D&D, D&D++ and OSD.

we constrain  $M_s^*$  to mimic the teacher  $M_s$ . So, we train  $M_s^*$  using the bias reducing classification loss  $L_{br}$  defined as

$$L_{br} = L_{class} + \lambda_2 L_{dis}, \quad (\text{A5})$$

where  $\lambda_2$  is used to weight  $L_{dis}$  in D&D++. We list the hyperparameters  $\lambda_1$  and  $\lambda_2$  in Table A2.

### A2.2. OSD

We construct a baseline called One Step Distillation (OSD) by skipping Step 2 of D&D++. Here, we first train a teacher network  $M_t$  that is trained on only one category of attribute  $A$  (category  $a_1$ ). Then, we initialize a new student network  $M_s^*$  and train it on both attribute categories of  $A$ . During this phase, we constrain  $M_s^*$  to mimic  $M_t$ . To realize this, we feed the given image to both  $M_s^*$  and  $M_t$  and obtain features  $f_s^*$  and  $f_t$ , respectively and compute their cosine distance using  $L_{dis}$

$$L_{dis}(f_t, f_s^*) = 1 - \frac{f_t \cdot f_s^*}{\|f_t\| \|f_s^*\|}. \quad (\text{A6})$$

Combining  $L_{dis}$  with  $L_{class}$ , we train  $M_s^*$  with a bias reducing classification loss  $L_{br}$  defined as

$$L_{br} = L_{class} + \lambda_{osd} L_{dis}, \quad (\text{A7})$$

where  $\lambda_{osd}$  is used to weight  $L_{dis}$  in OSD. The difference between D&D++ and OSD is that in D&D++,  $M_s^*$  uses a teacher ( $M_s$ ) that has information about both of the attribute categories, whereas in OSD,  $M_s^*$  uses a teacher ( $M_s$ ) with information about only one category.

We provide the hyperparameter  $\lambda_{osd}$  in Table A2. For all the steps in training networks in D&D, D&D++ and OSD, we use a batch size of 128. We train the networks for 300 epochs. We start with a learning rate of 0.1 and reduce the learning rate by 10% after every fifty epochs. We use SGD for optimization.

## A3. Detailed results

### A3.1. Results with Crystalface

In Tables 2, 3 and Figure 4 of the main paper, we provide detailed bias analysis of Crystalface and its de-

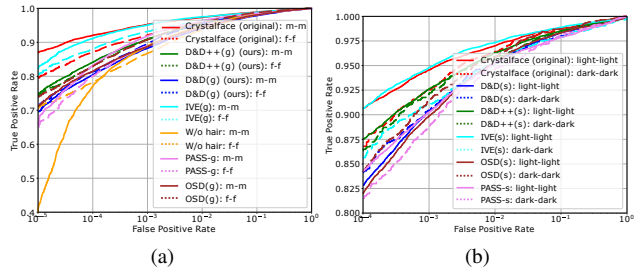


Figure A1. (a) Gender-wise verification plots for Crystalface and its gender-debiasing counterparts. ‘m-m’=male-male pairs, ‘f-f’=female-female pairs (b) Skintone-wise verification plots for Crystalface and its skintone-debiasing counterparts.

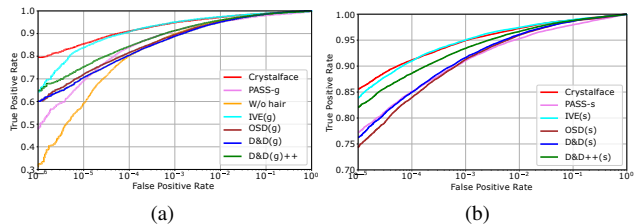
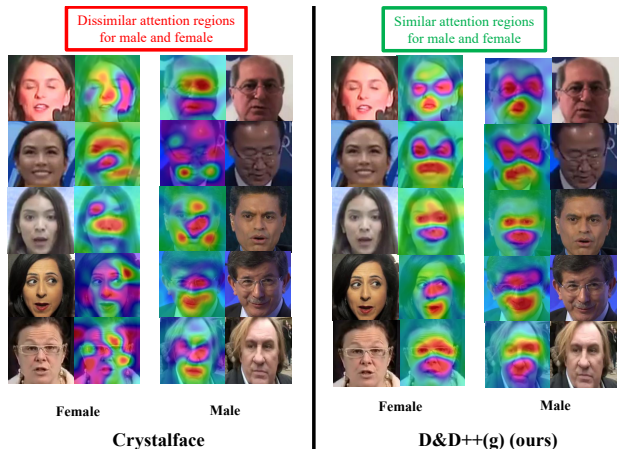


Figure A2. Overall verification plots for IJB-C dataset obtained using Crystalface and its (a) Gender-debiasing, and (b) Skintone debiasing counterparts.

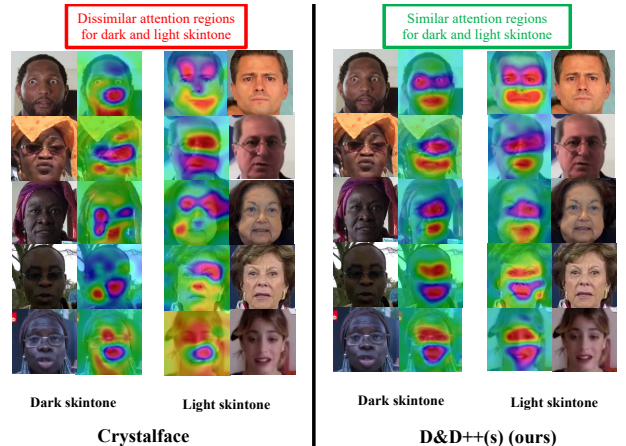
biasing counterparts. We report the gender bias analysis at  $FPR = 10^{-5}, 10^{-4}, 10^{-3}$  and skintone bias analysis at  $FPR = 10^{-4}, 10^{-3}, 10^{-2}$ , as done in [15]. Here, we provide the gender-wise and skintone-wise verification ROCs on IJB-C obtained using all of these methods in Figure A1. We also provide the overall verification ROCs (using all the pairs defined in the IJB-C 1:1 verification protocol [37]) obtained using Crystalface and its gender and skintone debiasing counterparts in Figure A2. In Figure 4 of the main paper, it should also be noted that our proposed baseline OSD obtains lower BPC than other baselines at most FPRs. This is because OSD (like D&D variants) also enforces the network to process the faces with attribute  $A = a_1$  and  $A = a_2$  in a similar way, by mimicking a teacher network that is trained on a single attribute category ( $A = a_1$ ). However, D&D and D&D++ considerably outperform OSD and other baselines in bias reduction. Also, in Figure 5 of the main paper, we provide some qualitative results for our best performing method D&D++, showing that a network trained with D&D++ attends to similar face regions for both categories of the binary attribute under consideration. Here, we show more of such qualitative examples in Figure A3.

### A3.1.1 Results on multiple skintones

A sensitive attribute may have more than two categories. In our context, the skintone attribute consists of three cate-



(a) Attention maps for male and female faces generated with D&D++(g) are more similar, that those generated with the original Crystalface network.



(b) Attention maps for faces with dark and light skintone generated with D&D++(s) are more similar, that those generated with the original Crystalface network.

Figure A3. D&D++ enforces the networks to attend to similar face regions for both categories of the binary attribute.

gories: Light, medium, dark. In Eq. 2 of the main paper, we chose to define skintone bias as the difference between the verification TPRs of light-light and dark-dark pairs at a given FPR. Following other works such as [56, 60] we can also define skintone bias as the standard deviation (STD) among the verification TPRs of light-light pairs, medium-medium pairs and dark-dark pairs. In Table A3, we report these STD values for the D&D systems (and the corresponding baselines) trained on Crystalface features, along with the average of the TPRs obtained for the three skintone categories. We find that our proposed D&D/D&D++ systems obtain considerably lower STD than existing baselines, thus mitigating skintone bias. We also provide the skintone-wise verification plots for all three skintones (light, medium and dark) on IJB-C dataset in Figure A6.

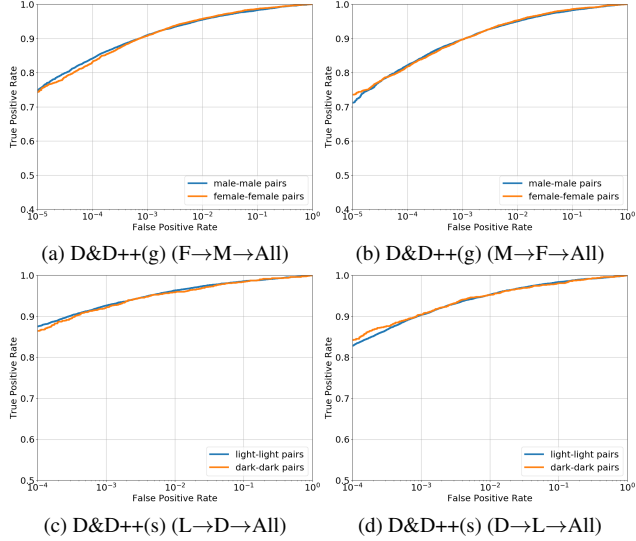


Figure A4. (a,b) Reversing the sequence in which different genders are learned in Crystalface-based D&D++(g). Here F=female and M=male subset of BUPT-BalancedFace dataset. (c,d) Reversing the sequence in which different skintones are learned in Crystalface-based D&D++(s). Here L=light and D=dark subset of BUPT-BalancedFace dataset.

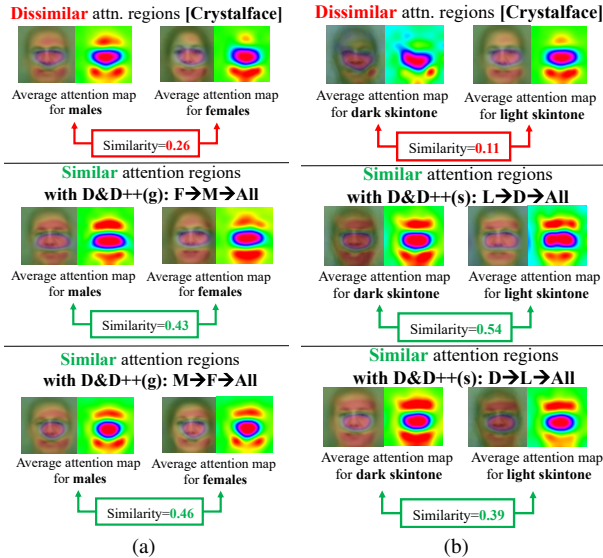


Figure A5. (a). D&D++(g) and reverse-ordered D&D++(g) generate more similar attention maps for male and female frontal faces, as compared to Crystalface. (b). D&D++(s) and reverse-ordered D&D++(s) generate more similar attention maps for dark and light frontal faces, than Crystalface.

### A3.1.2 Reversing the order in D&D++

In Section 5.4.3 (Table 4) of the main paper we discuss the effect of reversing the order in which different genders are learned in D&D++(g). We provide the detailed results for this experiment in Table A4 (top row). The gender-wise verification plots on IJB-C dataset for both D&D++(g) trained

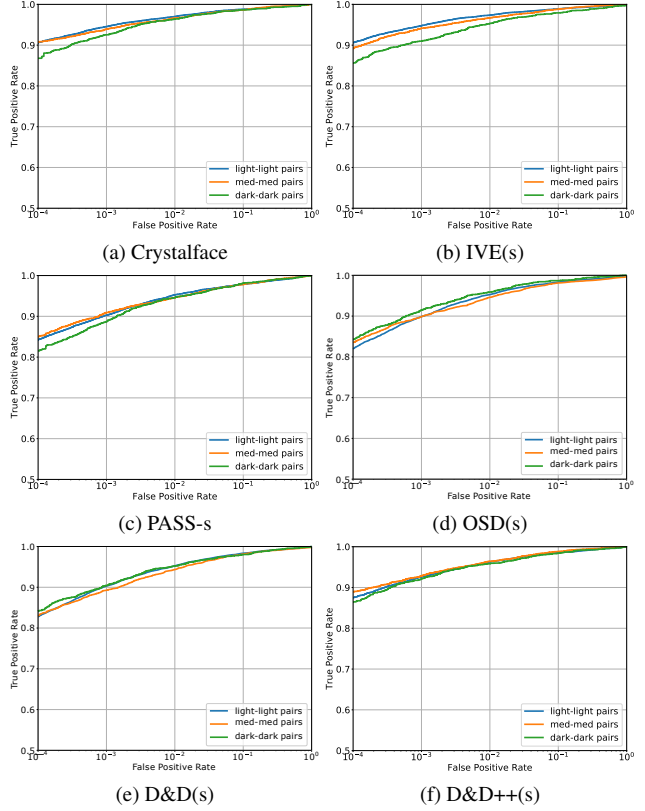


Figure A6. Skintone-wise verification ROCs for all three skintones (light, medium, dark) in IJB-C for Crystalface and its de-biasing counterparts.

with sequence Female(F)→Male(M)→All and that with sequence Male(M)→Female(F)→All are provided in Figures A4a and A4b respectively. We perform the same experiment with respect to the skintone attribute by reversing the order in which different skintones are learned in D&D++(s) and present the results in Table A4 (bottom row). The skintone-wise verification plots on IJB-C dataset for both D&D++(s) trained with sequence Light(L)→Dark(D)→All and that with sequence Dark(D)→Light(L)→All are provided in Figure A4c and A4d respectively. Additionally, in Fig. A5, we also provide the average attention maps for frontal male and female faces (generated by D&D++(g) and reverse-ordered D&D++(g)), and for frontal faces with light and dark skintone (generated by D&D++(s) and reverse-ordered D&D++(s)).

### A3.2. Results with ArcFace

As mentioned in Section 5.5 (Tables 5,6 and Figure 7) of the main paper, we apply D&D, D&D++ and all other de-biasing baselines on the Resnet-50 version of Arcface [11] to evaluate their generalizability. The gender bias analysis and skintone bias analysis for all the methods are provided

FPR	$10^{-4}$					$10^{-3}$					$10^{-2}$				
Method	TPR <sub>l</sub>	TPR <sub>med</sub>	TPR <sub>d</sub>	Avg	STD (↓)	TPR <sub>l</sub>	TPR <sub>med</sub>	TPR <sub>d</sub>	Avg	STD (↓)	TPR <sub>l</sub>	TPR <sub>med</sub>	TPR <sub>d</sub>	Avg	STD (↓)
Crystalface	0.906	0.906	0.867	0.893	0.018	0.945	0.939	0.925	0.936	0.008	0.970	0.968	0.963	0.967	0.003
IVE(s) <sup>†</sup> [55]	0.906	0.889	0.854	0.883	0.022	0.948	0.941	0.909	0.933	0.017	0.974	0.967	0.953	0.965	0.009
PASS-s) <sup>†</sup> [15]	0.842	0.844	0.815	0.834	0.013	0.903	0.904	0.886	0.898	0.008	0.953	0.946	0.946	0.948	0.003
OSD(s)	0.819	0.834	0.841	0.831	<u>0.009</u>	0.899	0.899	0.913	0.904	<u>0.007</u>	0.953	0.947	0.959	0.953	0.005
D&D(s)	0.828	0.829	0.839	0.832	<b>0.005</b>	0.903	0.889	0.904	0.899	<u>0.007</u>	0.953	0.948	0.952	0.951	<b>0.002</b>
D&D++(s)	0.875	0.888	0.862	0.875	0.011	0.926	0.927	0.921	0.925	<b>0.003</b>	0.963	0.963	0.959	0.962	<b>0.002</b>

Table A3. Average and Standard deviation (STD) among the verification TPRs of light-light pairs, medium-medium pairs and dark-dark pairs. TPR: overall True Positive rate, TPR<sub>l</sub>: light-light TPR, TPR<sub>med</sub>: medium-medium TPR, TPR<sub>d</sub>: dark-dark TPR. **Bold**=Best, Underlined=Second best. D&D variants obtain the lowest STD (bias) among the performance of the three skintones. <sup>†</sup>=Our implementation of baselines (See Sections A4, A5, A6 for details). All methods are trained on BUPT-BalancedFace [56] data.

FPR	$10^{-5}$					$10^{-4}$					$10^{-3}$				
Sequence	TPR	TPR <sub>m</sub>	TPR <sub>f</sub>	Bias(↓)	BPC <sub>g</sub> (↑)	TPR	TPR <sub>m</sub>	TPR <sub>f</sub>	Bias(↓)	BPC <sub>g</sub> (↑)	TPR	TPR <sub>m</sub>	TPR <sub>f</sub>	Bias(↓)	BPC <sub>g</sub> (↑)
F→M→All	0.754	0.744	0.741	0.002	<b>0.854</b>	0.844	0.841	0.830	0.011	0.701	0.914	0.910	0.907	0.002	0.898
M→F→All	0.703	0.711	0.735	0.024	0.501	0.813	0.821	0.817	0.004	<b>0.809</b>	0.893	0.897	0.897	0	<b>0.940</b>

FPR	$10^{-4}$					$10^{-3}$					$10^{-2}$				
Sequence	TPR	TPR <sub>l</sub>	TPR <sub>d</sub>	Bias(↓)	BPC <sub>st</sub> (↑)	TPR	TPR <sub>l</sub>	TPR <sub>d</sub>	Bias(↓)	BPC <sub>st</sub> (↑)	TPR	TPR <sub>l</sub>	TPR <sub>d</sub>	Bias(↓)	BPC <sub>st</sub> (↑)
L→D→All	0.886	0.875	0.862	0.013	<b>0.629</b>	0.934	0.926	0.921	0.005	<b>0.733</b>	0.967	0.963	0.959	0.004	<b>0.327</b>
D→L→All	0.849	0.839	0.827	0.012	0.615	0.913	0.908	0.897	0.010	0.461	0.951	0.956	0.950	0.006	-0.023

Table A4. Reversing the order in which different genders/skintones are learned in (top) D&D++(g) and (bottom) D&D++(s). Here, L=light and D=dark skintone subset of BUPTBalancedFace. Similarly, F=female and M=male subset of the dataset. ‘All’ refers to the entire dataset, required for training step 3 of D&D++.

in Tables A5 and A6, respectively. In Figure A8, we provide the gender-wise and skintone-wise ROCs in IJB-C for ArcFace and its debiasing counterparts. The overall verification ROCs (using all the pairs defined in the IJB-C 1:1 verification protocol [37]) are presented in Figure A9. We also provide qualitative results in Fig. A7 to show that D&D++ helps the network attend to similar spatial regions for both categories of the binary attribute under consideration.

### A3.2.1 Comparison with Debface [21]

In Tables 2, 3, 5, and 6 of the main paper we compare D&D++ with other methods including the recently proposed adversarial method PASS [15], and show that D&D++ consistently obtains higher face verification performance and lower bias than PASS. We note that DebFaceID [21] is another adversarial method proposed for removing protected attributes like gender and race from face representations, that uses a ResNet50 ArcFace backbone (similar to our ArcFace based D&D++). For the IJB-C dataset, this work reports the overall face verification performance. So, in Table A7, we compare the overall face verification performance obtained by D&D++ with that obtained by DebfaceID on IJB-C. D&D++ obtains higher face verification performance than DebfaceID at most FPRs. It should be noted that DebfaceID uses MS-Celeb-1M (MS1M) dataset [24] for training, which consists of approximately five million images, whereas D&D-based systems are trained on the

BUPT-BalancedFace dataset that consists of  $\sim 1.2$  million images. We do not use MS1M dataset as it does not contain race labels. On the other hand, BUPT-BalancedFace [56] contains race labels, making it easier to train skintone-debiasing models.

### A3.3. Bias v/s face verification performance

An ideal de-biasing system must reduce bias and maintain reasonable face verification performance. In Figure 8 of the main paper, we show the TPR at a fixed FPR and gender/skintone bias for several de-biasing methods, including our proposed methods. We fixed the FPR= $10^{-4}$  for gender de-biasing methods, and FPR= $10^{-3}$  for skintone de-biasing methods. Here in Figure A10, we provide the same plots for all the other FPRs. In these plots, an ideal de-biasing method would occupy the upper-left-hand corner, where the face verification performance is high, and bias is low, whereas in the worst case scenario, the de-biasing method would occupy the lower left corner which indicates high bias and low face verification performance.

## A4. Training details for PASS [15]

### A4.1. Brief summary of PASS

PASS [15] is composed of three components: (1) **Generator model  $M$** : A model that accepts face recognition feature  $f_{in}$  from a pre-trained network, and generates

FPR	$10^{-5}$					$10^{-4}$					$10^{-3}$				
	Method	TPR	TPR <sub>m</sub>	TPR <sub>f</sub>	Bias(↓)	BPC <sub>g</sub> (↑)	TPR	TPR <sub>m</sub>	TPR <sub>f</sub>	Bias(↓)	BPC <sub>g</sub> (↑)	TPR	TPR <sub>m</sub>	TPR <sub>f</sub>	Bias(↓)
ArcFace	0.879	0.884	0.841	0.042	0.00	0.914	0.922	0.890	0.032	0.00	0.944	0.946	0.928	0.017	0
IVE(g)† [55]	0.877	0.884	0.843	0.041	0.021	0.913	0.920	0.886	0.034	-0.064	0.944	0.944	0.927	0.017	0
W/o hair† [1]	0.726	0.412	0.821	0.409	-8.91	0.883	0.794	0.888	0.094	-1.97	0.926	0.930	0.926	<u>0.004</u>	<u>0.746</u>
PASS-g† [15]	0.798	0.681	0.768	0.087	-1.162	0.869	0.851	0.862	0.011	<u>0.607</u>	0.909	0.916	0.902	0.013	0.198
OSD(g)	0.778	0.758	0.780	0.022	0.361	0.848	0.849	0.865	0.017	0.397	0.898	0.901	0.917	0.016	0.010
D&D(g)	0.759	0.754	0.769	<u>0.016</u>	<u>0.483</u>	0.830	0.833	0.843	<u>0.010</u>	0.596	0.889	0.889	0.897	0.009	0.412
D&D++(g)	0.825	0.803	0.800	<b>0.002</b>	<b>0.891</b>	0.880	0.879	0.870	<b>0.009</b>	<b>0.682</b>	0.920	0.920	0.918	<b>0.002</b>	<b>0.857</b>

Table A5. *Gender* bias analysis for *ArcFace* network, and its de-biased counterparts on IJB-C. TPR: overall True Positive rate, TPR<sub>m</sub>: male-male TPR, TPR<sub>f</sub>: female-female TPR. **Bold**=Best, Underlined=Second best. D&D variants obtain higher BPC<sub>g</sub> and lower gender bias at most FPRs. †=Our implementation of baselines (See Sections A4, A5, A6 for details). All methods are trained on BUPT-BalancedFace [56] data.

FPR	$10^{-4}$					$10^{-3}$					$10^{-2}$				
	Method	TPR	TPR <sub>l</sub>	TPR <sub>d</sub>	Bias(↓)	BPC <sub>st</sub> (↑)	TPR	TPR <sub>l</sub>	TPR <sub>d</sub>	Bias(↓)	BPC <sub>st</sub> (↑)	TPR	TPR <sub>l</sub>	TPR <sub>d</sub>	Bias(↓)
ArcFace	0.914	0.912	0.883	0.029	0	0.944	0.942	0.922	0.021	0	0.964	0.964	0.950	0.014	0
IVE(s)† [55]	0.913	0.911	0.871	0.040	-0.380	0.943	0.941	0.919	0.022	-0.049	0.964	0.962	0.951	0.011	0.214
PASS-s† [15]	0.786	0.778	0.738	0.041	-0.554	0.861	0.859	0.846	0.014	0.245	0.920	0.921	0.922	<b>0.001</b>	<b>0.883</b>
OSD(s)	0.877	0.864	0.859	<u>0.005</u>	<u>0.787</u>	0.923	0.918	0.901	0.016	0.216	0.956	0.953	0.944	0.009	0.349
D&D(s)	0.855	0.836	0.851	0.015	0.418	0.913	0.906	0.895	<b>0.011</b>	<u>0.443</u>	0.951	0.947	0.942	0.005	0.629
D&D++(s)	0.882	0.871	0.868	<b>0.003</b>	<b>0.862</b>	0.926	0.923	0.912	<b>0.011</b>	<b>0.457</b>	0.957	0.954	0.951	<u>0.003</u>	<u>0.778</u>

Table A6. *Skintone* bias analysis for *ArcFace* network, and its de-biased counterparts on IJB-C. TPR: overall True Positive rate, TPR<sub>l</sub>: light-light TPR, TPR<sub>d</sub>: dark-dark TPR. **Bold**=Best, Underlined=Second best. D&D variants obtain higher BPC<sub>st</sub> and lower skintone bias at most FPRs. †=Our implementation of baselines (See Sections A4, A5, A6 for details). All methods are trained on BUPT-BalancedFace [56] data.

Method/FPR	$10^{-5}$	$10^{-4}$	$10^{-3}$	Training attributes	Dataset
Debface-ID	0.820	0.881	0.895	Race,age,gender	MS1M
D&D++(g)	0.825	0.880	0.920	Gender	BUPT-BF
D&D++(s)	0.823	0.882	0.926	Race	BUPT-BF

Table A7. ArcFace-based D&D++ v/s Debface [21]. Debface-ID numbers are obtained from the original paper [21].

a lower dimensional feature  $f_{out}$  that is supposed to be agnostic to sensitive attribute (gender or skintone).  $M$  consists of a single linear layer, followed by a PReLU [27] layer.

(2) **Classifier  $C$** : A classifier that takes in  $f_{out}$  and generates a prediction vector for identity classification.

(3) **Ensemble of attribute classifiers  $E$** : An ensemble of  $K$  attribute prediction models. Each of these models is a two layer MLP with 128 and 64 hidden units respectively with SELU activations, followed by a sigmoid activated output layer with  $N_{att}$  units, where  $N_{att}$  = the number of classes in the attribute being considered.

We use the official implementation of PASS [14] to build PASS-g (for reducing gender information in face recognition feature) and PASS-s (for reducing skintone information). We provide a brief summary of PASS training, and specify the hyperparameters used. More details are provided in the original paper [15]

**Stage 1 - Initializing and training  $M$  and  $C$** : Using input

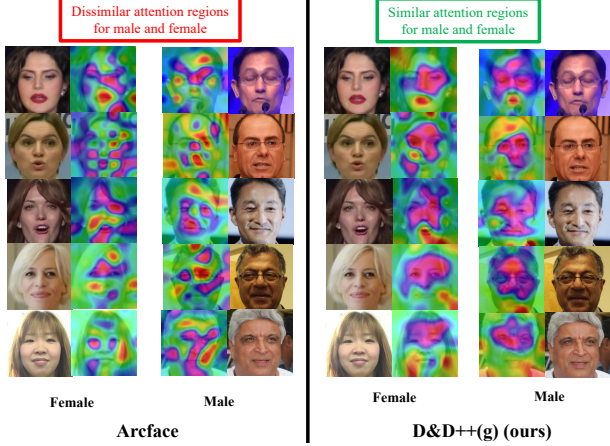
features  $f_{in}$  from a pre-trained network, we train  $M$  and  $C$  from scratch for  $T_{fc}$  iterations using  $L_{class}$ .  $L_{class}$  is the standard cross entropy classification loss. The learning rate used to train  $M$  and  $C$  in this stage is denoted by  $\alpha_1$ .

**Stage 2 - Initializing and training  $E$** : Once  $M$  is trained to perform classification, we feed the outputs  $f_{out}$  of  $M$  to ensemble  $E$  of  $K$  attribute prediction models.  $E$  is then trained to classify attribute for  $T_{atrain}$  iterations using  $L_{att}$ .  $L_{att}$  is a cross-entropy classification loss for classifying attributes. The learning rate used to train the models in  $E$  in this stage is denoted by  $\alpha_2$ . Model  $M$  remains frozen in this step.

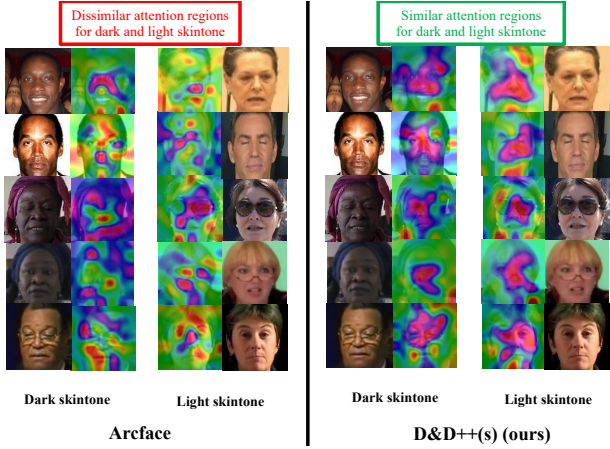
**Stage 3 - Update model  $M$  and classifier  $C$** : Here,  $M$  is trained to generate features  $f_{out}$  that can classify identities and have reduced encoding of sensitive attribute under consideration. We feed  $f_{out}$  to  $E$  and  $C$ , the outputs of which result in an adversarial de-biasing loss  $L_{deb}$  and  $L_{class}$  respectively. We combine them to compute the bias reducing classification loss in PASS denoted as  $L_{br}^{(PASS)}$

$$L_{br}^{(PASS)} = L_{class} + \lambda L_{deb}, \quad (A8)$$

$L_{br}^{(PASS)}$  is used for training  $M$  and  $C$  for  $T_{deb}$  iterations, while  $E$  remains locked.  $\lambda$  is used to weight the adversarial loss  $L_{deb}$ . The learning rate used to train  $M$  and  $C$  in this stage is denoted by  $\alpha_3$ .



(a) Attention maps for male and female faces generated with D&D++(g) are more similar, that those generated with the original Arcface network.



(b) Attention maps for faces with dark and light skintone generated with D&D++(s) are more similar, that those generated with the original Arcface network.

Figure A7. D&D++ enforces the networks to attend to similar face regions for both categories of the binary attribute.

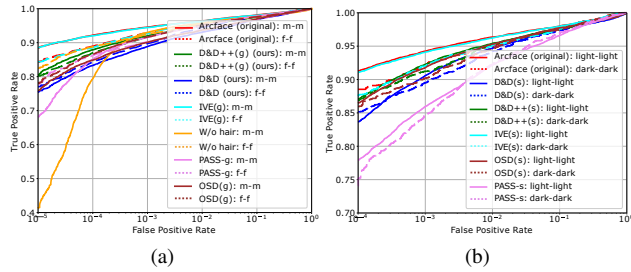


Figure A8. (a) Gender-wise verification plots for ArcFace and its gender-debiasing counterparts. ‘m-m’=male-male pairs, ‘f-f’=female-female pairs (b) Skintone-wise verification plots for ArcFace and its skintone-debiasing counterparts

**Stage 4 - Update ensemble  $E$  (discriminator):** In stage 4, members of  $E$  are trained to classify attribute using  $f_{out}$ .

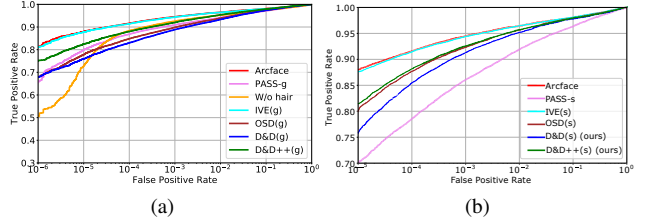


Figure A9. Overall verification plots for IJB-C dataset obtained using ArcFace and its (a) Gender-debiasing, and (b) Skintone-debiasing counterparts

Backbone		Crystalface		ArcFace	
Hyperparam	Stage	PASS-g	PASS-s	PASS-g	PASS-s
$\lambda$	3	1	10	10	10
$K$	2, 3, 4	4	2	3	2
$T_{fc}$	1	16000	16000	10000	10000
$T_{deb}$	3	1200	1200	1200	1200
$T_{atrain}$	2	30000	30000	30000	30000
$T_{plat}$	4	2000	2000	2000	2000
$A^*$	4	0.90	0.95	0.95	0.95
$\alpha_1$	1	$10^{-2}$	$10^{-2}$	$10^{-2}$	$10^{-2}$
$\alpha_2$	2,4	$10^{-3}$	$10^{-3}$	$10^{-3}$	$10^{-3}$
$\alpha_3$	3	$10^{-4}$	$10^{-4}$	$10^{-4}$	$10^{-4}$
$T_{ep}$	3,4	40	40	40	40

Table A8. Hyperparameters for training PASS-g and PASS-s on ArcFace and Crystalface features

So, stages 3 and 4 are run alternatively, for  $T_{ep}$  episodes, after which all the models in  $E$  are re-initialized and re-trained (as done in stage 2). Here, one episode indicates an instance of running stages 3 and 4 consecutively. In stage 4, following the discriminator-training strategy introduced by [15], we choose one of the models in  $E$ , and train it for  $T_{plat}$  iterations or until it reaches an accuracy of  $A^*$  on the validation set.  $M$  and  $C$  remain frozen in this stage.

#### A4.2. Datasets and Hyperparameters for PASS

In the original paper [15],  $f_{in}$  is obtained from a pre-trained Crystalface network that has been trained on a mixture of UMDFaces [7], UMDFaces-Videos [6] and MS1M [24]. Following this, the authors train PASS-g on the mixture dataset and PASS-s on BUPT-BalancedFace dataset. However, due to the current unavailability of the UMD-Faces and UMDFaces-Videos dataset and to make PASS variants comparable with D&D (and OSD) variants, we obtain  $f_{in}$  from a Crystalface network that has been trained on the BUPT-BalancedFace [56]. Then, we train both PASS-g and PASS-s on BUPT-BalancedFace as well.

We note that the authors of PASS [15] also perform experiments on Arcface. However, they perform experiments using the ResNet 101 version of the Arcface network. But,

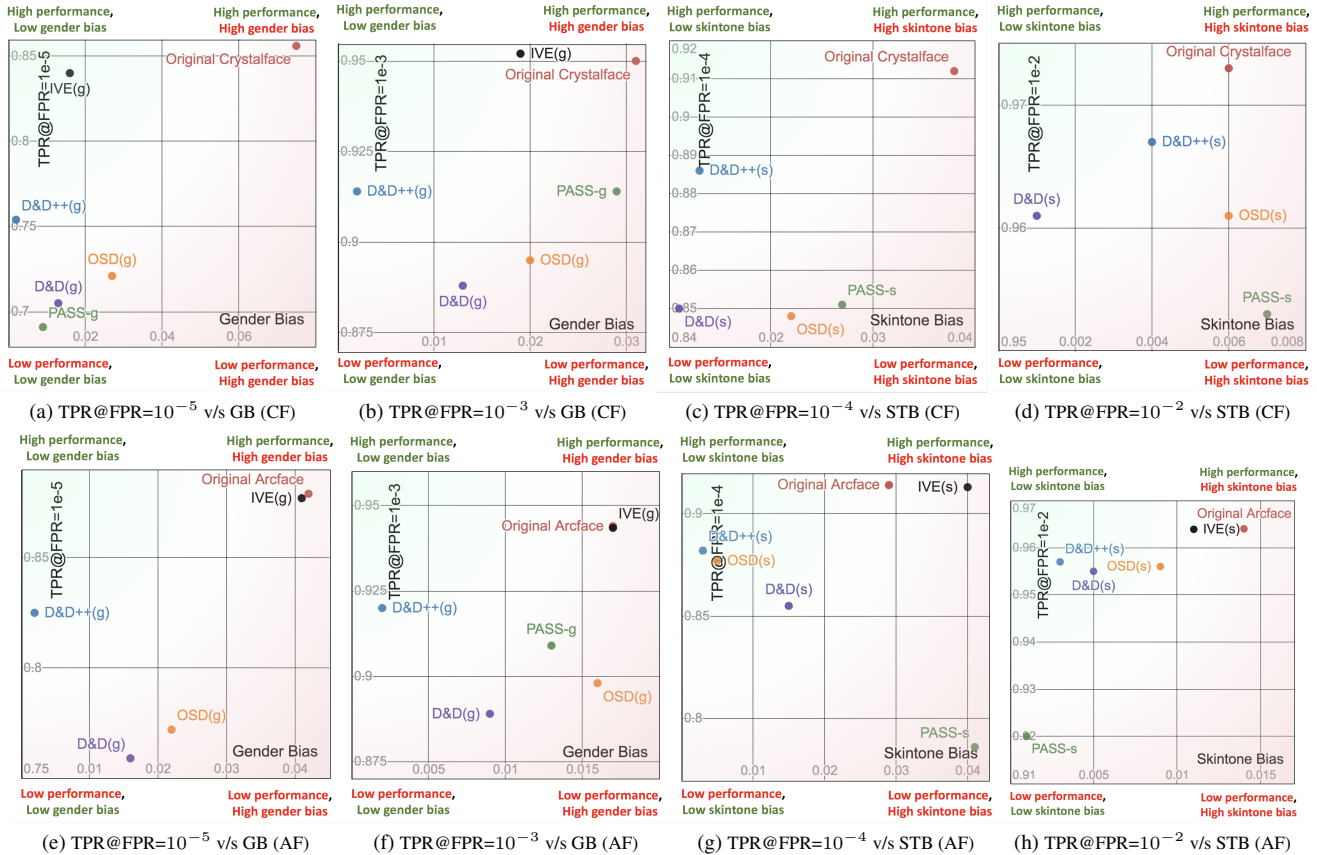


Figure A10. TPR at a fixed FPR (a,b) v/s Gender bias(GB) in Crystalface(CF) based models. (c,d) v/s Skintone bias(STB) in CF-based models. (e,f) v/s GB in Arcface(AF) based models. (g,h) v/s STB in AF-based models.

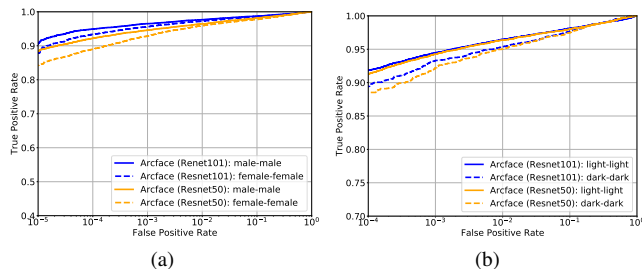


Figure A11. (a) Gender-wise and (b) Skintone-wise verification ROCs on the IJB-C dataset, for Resnet50 and Resnet101 version of the Arcface networks, trained on BUPT-BalancedFace dataset.

in our preliminary experiments, we found that the ResNet50 version of Arcface network demonstrate more gender and skintone bias, as shown in Figures A11 and A12. With this reasoning, and following some other previous works [21, 22], we use the Resnet 50 version of Arcface in our experiments, which is unlike the experiments in PASS [15].

We use the same hyperparameters specified in the original paper [15] and present them in Table A8. We use a batch size of 400 in all these experiments. In our work, we use the

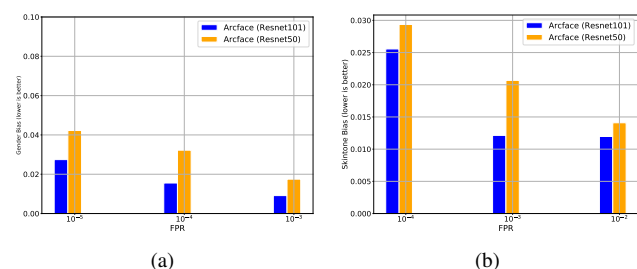


Figure A12. (a) Gender bias and (b) Skintone bias on the IJB-C dataset, demarcated by Resnet50 and Resnet101 version of the Arcface networks, trained on BUPT-BalancedFace dataset. Clearly, Resnet50 version of Arcface demonstrates more gender and skintone bias than its Resnet101 counterpart, which is why we use Resnet50 Arcface in our experiments, unlike [15]

official implementation of PASS [14].

## A5. Training details for IVE [55]

IVE [55] is an attribute suppression algorithm that assigns a score to each variable in face representations using a decision tree ensemble. This score of a variable indicates

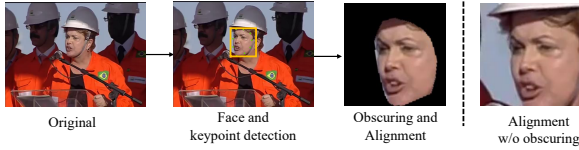


Figure A13. Our method for obscuring hair (Similar to [1]). On the right, we show an aligned image without obscuring hair.

the importance of that variable for a specific recognition task. Variables that affect attribute classification considerably are then excluded from the representation. In every exclusion step,  $n_e$  variables are removed from the representation. The algorithm is run for  $n_s$  steps, thus resulting in exclusion of  $n_s \times n_e$  variables from the representation. We follow the re-implementation of IVE by [15] and construct two variants of IVE: IVE(g) for reducing gender information and IVE(s) for reducing skintone information.

IVE is a feature-based system that reduces information of sensitive attribute from features obtained using a pre-trained network (like Crystalface or ArcFace). So before training IVE, we first train a Crystalface network on the BUPT-BalancedFace dataset. After that, we train IVE(g) and IVE(s) (separately) as follows:

**Training IVE(g)** : We extract Crystalface features for the images in BUPT-BalancedFace. We also obtain the gender labels for these images using [46]. Then we use the IVE system (explained in [55]) to remove variables in the features that encode gender information. During inference, we use the trained IVE(g) system to transform the Crystalface features extracted for the evaluation dataset (IJB-C).

**Training IVE(s)**: We follow the same experimental setup for training IVE(s). The only difference is that in IVE(s), instead of gender labels, we feed the race label (already provided in the BUPT-BalancedFace dataset) along with the Crystalface features extracted for the images in BUPT-BalancedFace dataset. For inference, we use the trained IVE(s) system to transform Crystalface features for IJB-C.

We perform the same experiment by replacing the pre-trained Crystalface network with an ResNet-50 ArcFace network trained on BUPT-BalancedFace dataset, for our ArcFace-based experiments. The official implementation for training IVE is publicly available [54]. In all of our IVE experiments, we use the parameters values mentioned in the code, i.e.  $n_s = 20$  and  $n_e = 5$ , thus resulting in 100 eliminations. Since face recognition features from ArcFace or Crystalface are 512-dimensional, the trained IVE(s/g) framework transforms the input features for test images into 412 dimensional features, which are then used to perform face verification.

## A6. Pipeline for obscuring hair

In [1], the authors obscure hair regions of images in the evaluation dataset. This is done to get an equal fraction of pixels in the images for each gender. The authors use a segmentation network [62] to obscure the hair. As a result of obscuring hair, it is shown that the resulting face recognition features extracted using ArcFace demonstrate lower gender bias. However, as pointed out by [15], such experiments are only performed on datasets with clean frontal faces in MORPH [48] and Notre-Dame [42] datasets. But, complex datasets like IJB-C contain varied and cluttered poses, which is why segmentation cannot be used (especially for images with extreme poses). So, following [15], we compute the face border keypoints using [46] and obscure all the regions outside the polygon formed by these keypoints. Our hair obscuring pipeline is presented in Fig A13. Note that, this baseline method cannot be used for mitigating skintone bias. After obscuring hair regions for images in the IJB-C dataset, we extract their features using pre-trained Crystalface/Arcface networks trained on BUPT-BalancedFace, and perform 1:1 face verification.